Seismic assessment of historical masonry towers by means of simplified approaches and standard FEM

Marco Valente, Gabriele Milani *

Department of Architecture, Built Environment and Construction Engineering, Politecnico di Milano, Piazza Leonardo da Vinci 32, 20133 Milano, Italy

The seismic vulnerability assessment of eight historical masonry towers, located in the North-East region of Italy, is carried out by means of simplified approaches. Three-dimensional finite element models of the eight towers are created on the basis of geometrical data deduced from both existing available documen-tation and insitu surveys. First, preliminary eigen-frequency analyses are performed in order to obtain some basic information about the structural behavior of the different towers. Then, a simplified approach based on non-linear static pushover analyses is adopted for the seismic verification of the global perfor-mance of the eight towers. In order to avoid unnecessary complications due to the utilization of ortho-tropic damaging models requiring many material parameters, a damage plasticity approach is used for masonry. The essential aspects of the masonry material are reproduced with sufficient care, namely the very low tensile strength, damage in tension and crack-crushing in compression. From an overall analysis of the results, it can be observed that almost all the towers are able to resist the seismic action corresponding to $Sa_g = 0.1$ g, whereas the majority are unsafe at least along one geometric direction for $Sa_g = 0.2$ g. Finally, this study presents the evaluation of the seismic safety Index by means of the simpli-fied sectional approach suggested by Italian Guidelines on Cultural Heritage. The collapse accelerations for the towers under consideration are compared and it is found that the results obtained with the dif-ferent approaches are in a good agreement with a slight conservative trend for the simplified procedure proposed by Italian Guidelines.

Keywords: Masonry towers, 3D FE models, Simplified assessment procedures, Pushover analyses, Seismic safety, Index

HIGHLIGHTS

- Non-linear 3D FE pushover analyses on eight existing masonry towers.
- Preliminary modal analyses on complex 3D FE discretizations.
- Comparison with simplified approaches suggested by Italian Guidelines on Cultural Heritage.
- Utilization of elasto damaging 3D models for seismic vulnerability evaluation.
- Comparative seismic analyses of masonry towers with different geometric features.

1. Introduction

Preservation of the architectural heritage is a fundamental issue in the cultural life of modern societies and the analysis of the historical masonry constructions is a challenging field of study. Masonry towers in form of medieval defence, clock and churches bell towers are quite diffused in Italy and are an important part of the historical and architectural heritage to be preserved. Recent seismic events have highlighted that ancient masonry towers are particularly susceptible to damage and prone to partial or total collapse under earthquake excitations. The safety assessment of these structures against earthquakes appears to be of relevant importance for historical, social and artistic reasons. Ancient masonry towers very often exhibit unique peculiar morphologic and typological characters, which might affect their structural behavior under horizontal loads.

In ancient times there was no instrument to design structures against earthquakes and towers do not represent an exception. As all other structures, they were usually conceived mainly to withstand vertical loads. Recently, however, national [1–3] and international standards [4] have imposed the evaluation of the

Article history:
Received 30 August 2015
Received in revised form 22 November 2015
Accepted 16 January 2016

* Corresponding author.
E-mail address: milani@stru.polimi.it (G. Milani).

structural performance in presence of horizontal loads, which simulate earthquake excitations, encouraging the use of sophisticated non-linear methods of analysis.

A detailed analysis of the documentation regarding the damages caused by recent and less recent Italian earthquakes [5–9] and direct insitu surveys allow to draw interesting conclusions on the qualitative behavior of masonry towers subjected to seismic actions. In particular, in isolated bell towers damage frequently develops along vertical cracks passing through openings, with concentration at the belfry level and at the base, suggesting a failure for combined effects of flexural and shear actions. When shear vertical cracks start to propagate, the validity of the Euler–Bernoulli hypothesis of plane cross-section does not hold anymore and therefore a full 3D FE analysis in the inelastic range is needed. Generally speaking, the damage evolution during a dynamic excitation plays a crucial role in modifying and reducing the resisting geometry of the structure, thus activating higher vibration modes [10].

According to the previous remarks, it is pretty clear that the most accurate approach to deal with the analysis of masonry towers under horizontal loads requires specific *ad hoc* FE devices [11–16] in order to deal with the complexity of the problem through a suitable level of accuracy.

Limiting the discussion to the masonry material, it is common opinion that at a macroscopic level, to be reliable, any model should take into account the essential aspects of brickwork, namely softening in both tension and compression, very low tensile strength and orthotropy in both the elastic and inelastic range. In addition, it is of paramount importance to model the different behavior in tension and compression that characterizes the masonry material. When dealing with non-linear dynamic analyses, a softening model with damage is also required to properly describe the dissipation of the seismic energy through repeated cycles of inelastic deformation [17]. When a tower is not particularly slender and depending on the frequency content of the earthquake excitation, flexural damages are always associated with significant shear cracks.

Orthotropic behavior is however less important when masonry texture is not well defined, as for historic structures and as extensively shown in [18–20], or in all those cases where there are multi-leaf walls or the structural behavior is mainly characterized by the vertical direction, as exactly occurs for towers. For this reason, it is not recommended, within the study of a tower, to model masonry by means of complex orthotropic models, where several coefficients must be set without any experimental/practical characterization. As a consequence, an isotropic softening model with both plastic deformation and damage is used in this study.

The paper presents comprehensive comparative results on the seismic performance assessment of eight historical masonry towers located in the North-East region of Italy, see Fig. 1. The towers exhibit different geometries in terms of slenderness, cross-section area, perforations, wall thicknesses and internal irregularities, but they show some affinities, as for instance the location and the similar masonry material, which allow for performing a comparative analysis of the results. Their structural behavior under horizontal loads may be therefore thought to be mainly influenced by geometrical issues.

All the towers are numerically analyzed by means of detailed full 3D FE models. The geometry of the towers is deduced from both existing available documentation and in situ surveys. On the basis of such geometrical data, a detailed 3D realistic mesh is conceived, with a point by point characterization of each single geometric element.

The seismic vulnerability of the eight towers under study is evaluated by means of different simplified procedures. The effectiveness of the use of different approaches for the seismic performance assessment of other typologies of structures is described in [21–24].

First, a standard eigen-frequency analysis is performed with the aim of identifying the vibration modes characterized by a high participating mass as well as the corresponding periods to compare with accelerations provided by code response spectra. Albeit approximate, because masonry exhibits a non-linear behavior even at very low levels of the external loads, such a standard approach may give a rough indication of the weaknesses of the structures that can be compared with more sophisticated methods of analysis.

Then, a simplified procedure based on non-linear static analyses is used for the seismic performance assessment of the masonry towers. Non-linear static analyses have recently assumed a large relevance, especially for the assessment of existing structures, according to code of practice requirements. A damage plasticity material exhibiting softening in both tension and compression, already available in the commercial code Abaqus [25], is adopted to model masonry. Global finite element pushover analyses are performed with different horizontal load distributions, according to Italian code requirements [1], along orthogonal (positive and negative) directions. The seismic assessment of the towers is carried out comparing the displacement capacity and demand. The

Fig. 1. Geographical location of the towers considered in this study, North-East region of Italy.

theoretical predictions are performed for two different (Sa_g = 0.1 g and Sa_g = 0.2 g) seismic intensity levels.

Finally, results are compared with the simplified procedure proposed by Italian Guidelines [3] on Cultural Heritage for the safety assessment of historical masonry towers in seismic zones. The seismic safety Index and the collapse acceleration for the different towers are evaluated and compared.

The paper is organized as follows: Section 2 provides a concise architectural description of the case studies, Section 3 describes the material model used for masonry in numerical simulations, whereas Sections 4–6 present the results of the simplified procedures applied in this study with a comparative discussion of the main outcomes.

2. Architectural description of the towers and FE models

In what follows, a concise architectural description of the towers (bell, clock or battle towers) under study is provided. A general view, the relevant geometrical features and the FE models of the eight towers are presented from Figs. 2 to 9.

2.1. Clock tower in Trecenta (Tower I)

Tower I, see Fig. 2, is a civic tower located in Trecenta, a small town between Rovigo and Mantua, in Veneto region. The tower is entirely built from masonry, with a regular texture. The height is about 22 m and the slenderness, defined as the ratio between the overall height of the structure and the smallest dimension of the base cross section, is roughly equal to 3.4. The tower is internally subdivided into six storeys, which are connected vertically by a wooden staircase. Each level is square in plan and consists of a unique space, which is partly occupied by the staircase. The ground floor is raised above the surrounding building through a slab with a thickness of 85 cm. For the first four floors the thickness of the perimeter walls is 110 cm, while for the last two is 90 cm. Most of the openings are located on the northern and southern façades.

Historical catalogues show that the strongest earthquake, in a radius of 30 km from the city, occurred on 20 May 2012 in Emilia Romagna (22.3 km far from Trecenta) with a magnitude M = 5.1. During the last 5 years (2009–2014), almost 500 earthquakes were

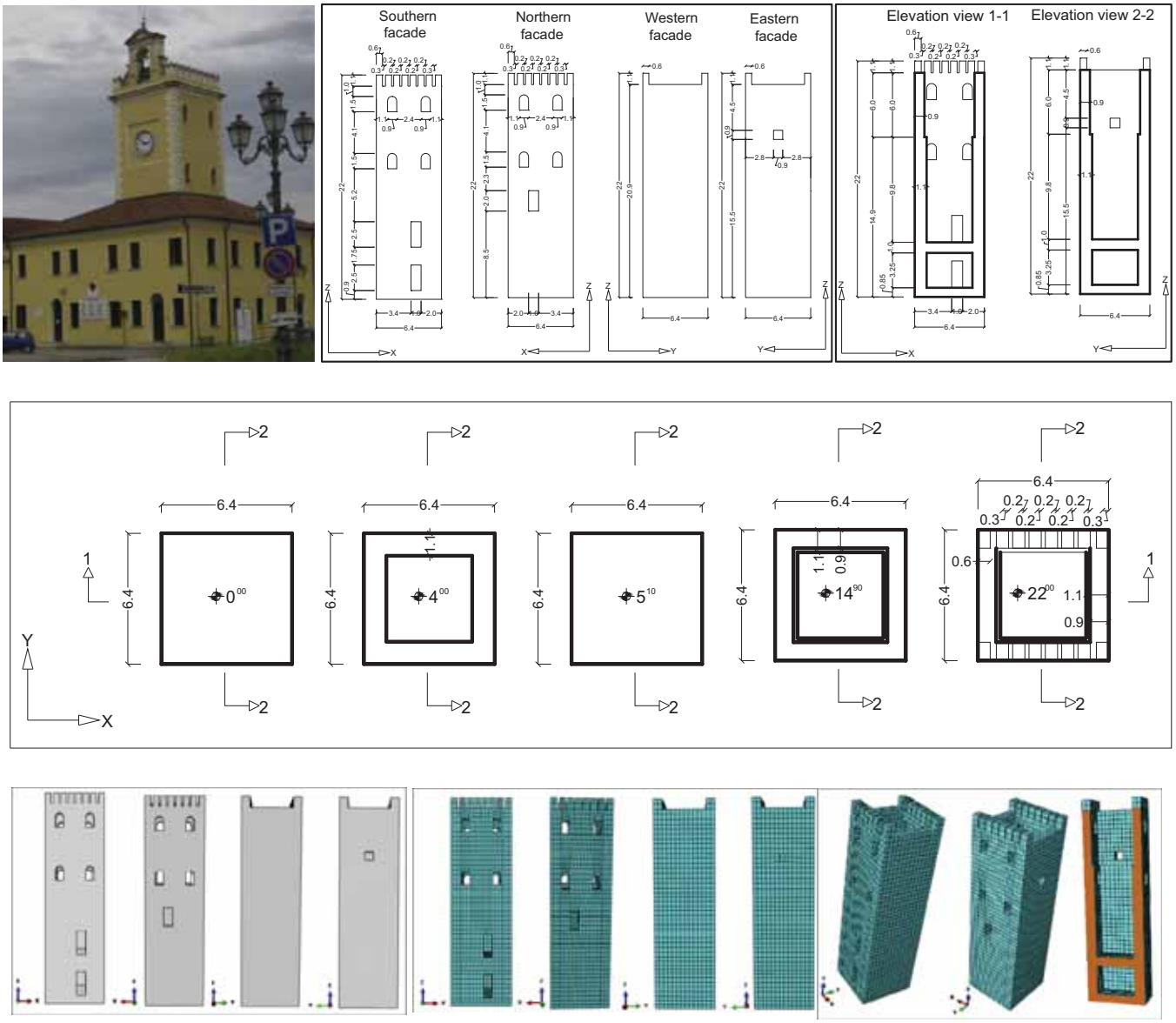

Fig. 2. Tower I, clock tower in Trecenta.

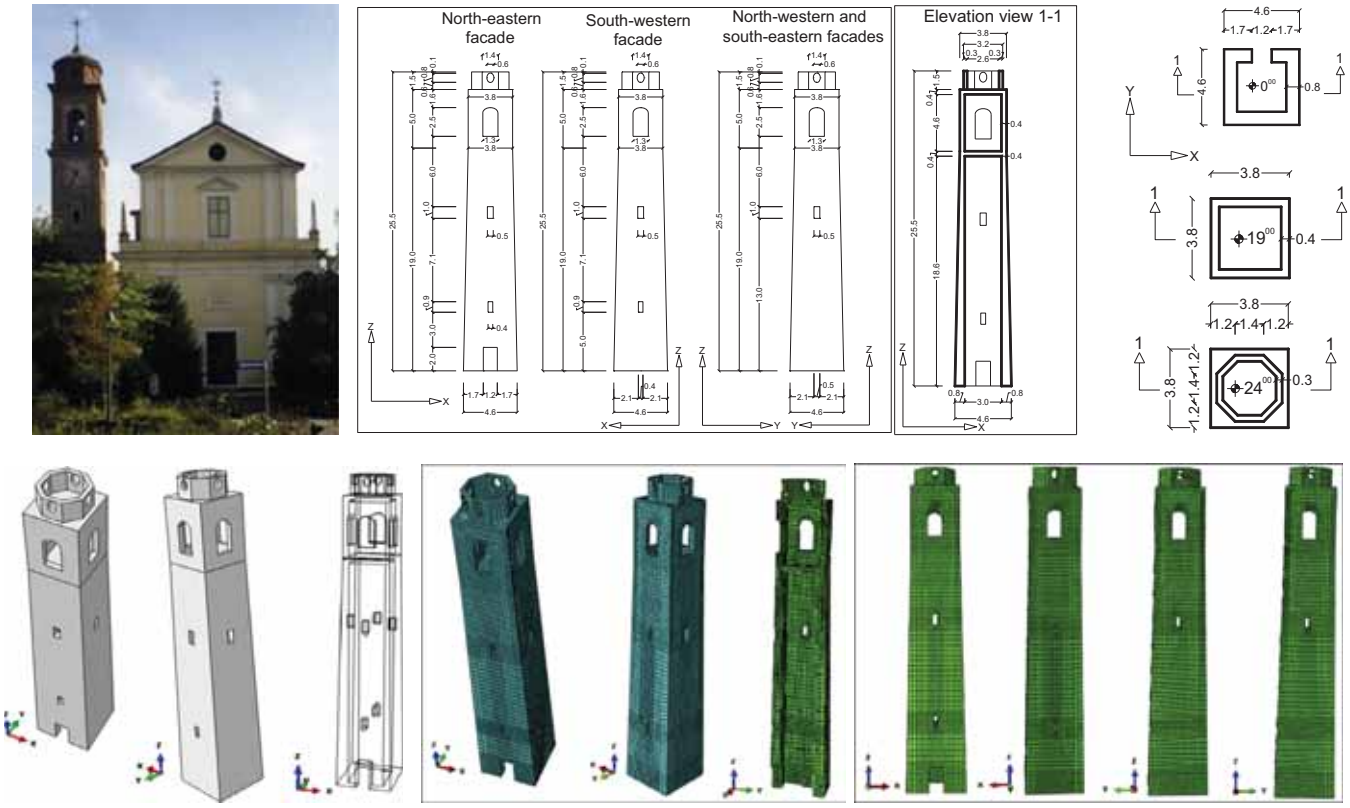

Fig. 3. Tower II, bell tower of San Giacomo church.

recorded within the given radius, all of them with a magnitude between 2 and 5.1. It is interesting to notice that some of the examples analyzed, as the present one, are not isolated towers but structures interconnected with churches or other building typologies, mainly between the ground and first floor level. Such geometric constraints cannot be taken into account easily in both non-linear static and non-linear dynamic analyses and the role that such constraints may play is complex and certainly beyond the scopes of the present paper. A preliminary comparative study has been conducted for the clock tower in Trecenta (Tower I), comparing the fundamental mode obtained with a FE discretization of the isolated tower and that derived from a FE model accounting for the whole built complex. As can be seen from Fig. 10 (and as expected), the difference in terms of both deformed shapes and values of the fundamental period found is not negligible, meaning that the utilization of isolated models, at least for the elastic properties of the constituent materials, should be done with particular care. The utilization of global models is therefore highly recommended and further research is obviously needed in the non-linear case, but this is not the object of the present paper, where a comparison among different geometries is done, without taking into consideration the real interconnections of the towers with neighboring structures.

2.2. Bell tower of San Giacomo church (Tower II)

Tower II, see Fig. 3, is a bell tower located in Polesine (Pegognaga), a small town in the province of Mantua in Lombardia region. Together with the church of San Giacomo Maggiore, it forms a complex of historical interest. During the recent Emilia-Romagna seismic event, it was severely damaged, with visible vertical cracks, a pattern that is typical for masonry towers subjected to horizontal loads. The bell tower, which dates back to the eighteenth century, has a square cross section with an external side of about 4.6 m. It presents an overall height of 25.5 m with a slenderness of about 5.5 and is internally subdivided into five floors. It was built entirely of regular small clay bricks with good mechanical properties. Walls, becoming gradually thinner from the bottom to the top, are 80 cm thick at the ground floor level and 40 cm at the top of the structure. Floors and stairs connecting the different levels are built from timber. Openings are present on all the façades. The structure is isolated, fully separated from the church, situated a few meters away. This feature excludes the possibility of any interaction between the two structures during the analysis under horizontal loads. As a consequence, the damage caused by the recent Emilia Romagna earthquake depends exclusively on the characteristics of the tower itself and on the seismic event. The damage reported after the event is mainly concentrated along vertical lines of weakness, located in correspondence with the openings that indeed are vertically aligned. The most relevant damage occurred on the North-East and the South-West parallel façades. After visual inspection, the texture appears extremely regular, with a good interconnection between perpendicular walls.

Historical catalogues show that the strongest earthquake, in a radius of 30 km far from the town, occurred at Concordia sulla Secchia (18.5 km far from Polesine) in 1346 with a magnitude $M = 5.81$, while the latest and strongest one occurred on 29 May 2012 in Emilia Romagna with magnitude $M = 5.8$. During the last 5 years (2009–2014) almost 1000 earthquakes were recorded within the given radius, all of them with a magnitude between 2 and 5.8.

2.3. Clock tower in Lendinara (Tower III)

Tower III, see Fig. 4, is a military city tower located in Lendinara, a town near Rovigo in Veneto region. The tower, which in ancient times represented the gate of the town, is nowadays the connection between two small squares. It has a height equal to about

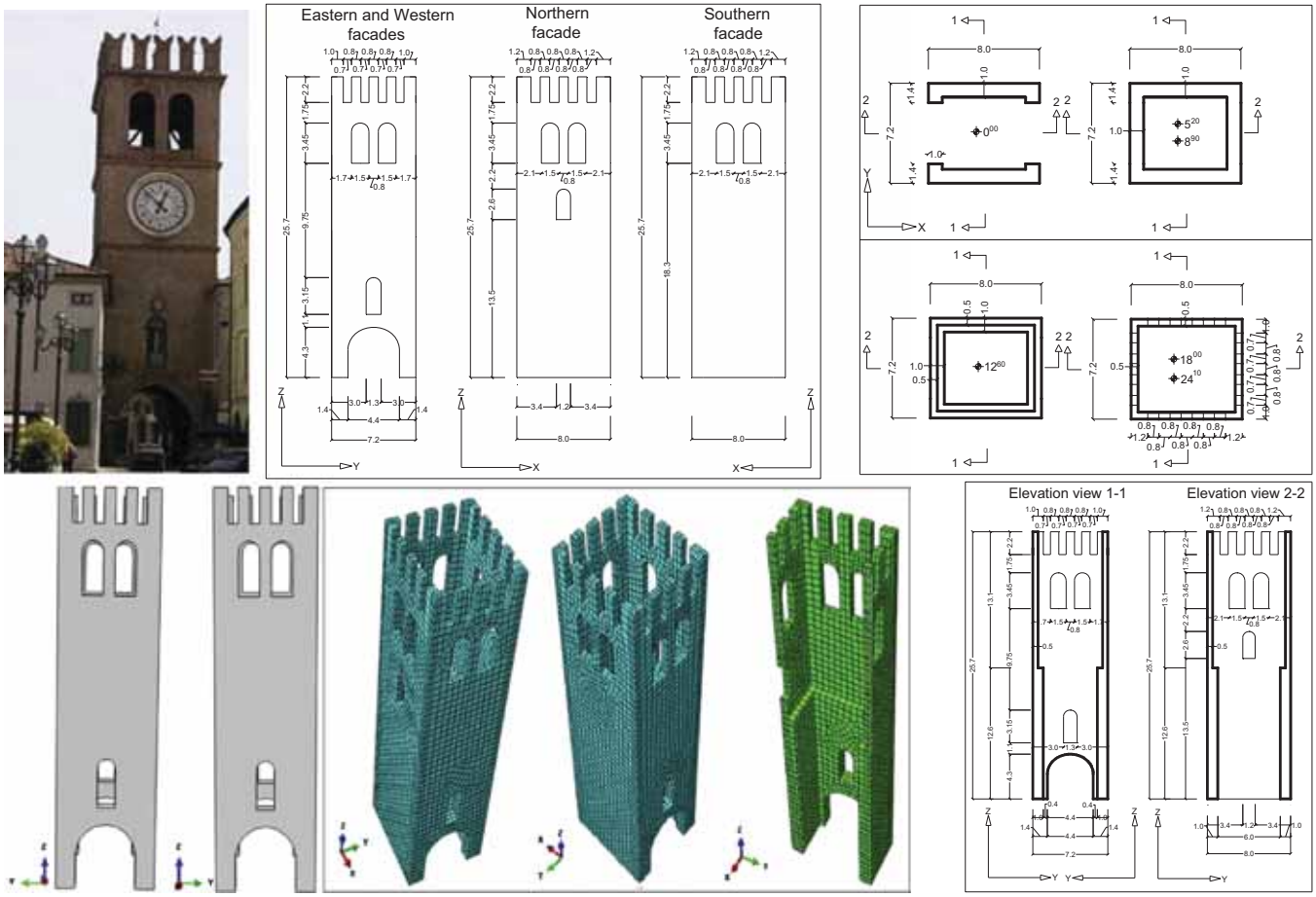

Fig. 4. Tower III, clock tower in Lendinara.

26 m and the slenderness is about 3.6. It exhibits an almost square plan and is internally subdivided into five storeys, plus one detectable mezzanine between the third and the fourth level. The tower is built entirely from bricks with a regular shape assembled in very regular texture. The thickness of the walls is equal to 100 cm for the first two floors and to 50 cm for the remaining part of the structure. The eastern and western façades are almost identical, both decorated with a clock and adorned with wooden frames and terracotta. It presents some internal irregularities for the presence of two arches at the ground floor, as depicted in Fig. 4. On the top there is a large double opening on each side of the structure. The tower is decorated by merlon elements, highlighted by a stylish notched frame. The structure needs some restoration interventions, especially to strengthen the floors and the roof.

The strongest earthquake, in a radius of 30 km far from the tower, occurred in 1234 in Ferrara (27.5 km far from Lendinara) with a magnitude $M = 5.17$. Such an earthquake is remembered as the most devastating for the city of Ferrara with the destruction of many important buildings, castles and churches. The latest destructive seismic event occurred again in occasion of the 2012 Emilia-Romagna seismic sequence, with a magnitude $M = 5.1$. During the last 5 years (2009–2014) almost 150 shakes were recorded within the given radius, all of them with a magnitude between 2 and 5.1.

2.4. Maistra tower of praetorian palace (Tower IV)

Tower IV, see Fig. 5, is located in Lendinara, as the previous one. The original tower was built in crenelated style, with clay bricks regular in shape. The tower has a height of 26.3 m and is one of the highest towers in the region of Polesine. The slenderness is about 2.9. In elevation the building is subdivided into five stories and there is a detectable mezzanine between the ground and the first floor, connected by a wooden staircase. The tower is almost square in plan and there is an internal subdivision into three rooms – two small ones and a hallway. All the ceilings are made of wood boards, but only the first floor has its original terracotta tiles. The thickness of the walls is 155 cm and is constant along the height of the tower. The structure stands on a tapering upwards base. The openings of the ground, mezzanine and first floors are small and have square shape. In the past the tower was crowned by merlon elements (found in several ancient maps).

2.5. Tower of Treves castle (Tower V)

Tower V, see Fig. 6, is located in Arquà Polesine, a small town between the cities of Rovigo and Ferrara in Veneto region. The tower, which dates back to the 12th century and belongs to Este castle (now Treves castle), received some important amendments during the centuries but globally preserves its original medieval character. The height of the structure is around 24 m and the slenderness is about 3.3. Vertically, the internal space is subdivided into four storeys, connected by a narrow stone-made stair. Each storey has a square plan, consisting of a single compartment and a barrel-vaulted ceiling. The thickness of the walls changes in correspondence with each level as follows: 160 cm, 120 cm, 100 cm and 80 cm on the ground, first, second and third floor respectively. Some of the arches and the windows of the original design are now buffered and others have been modified. On the third floor of the

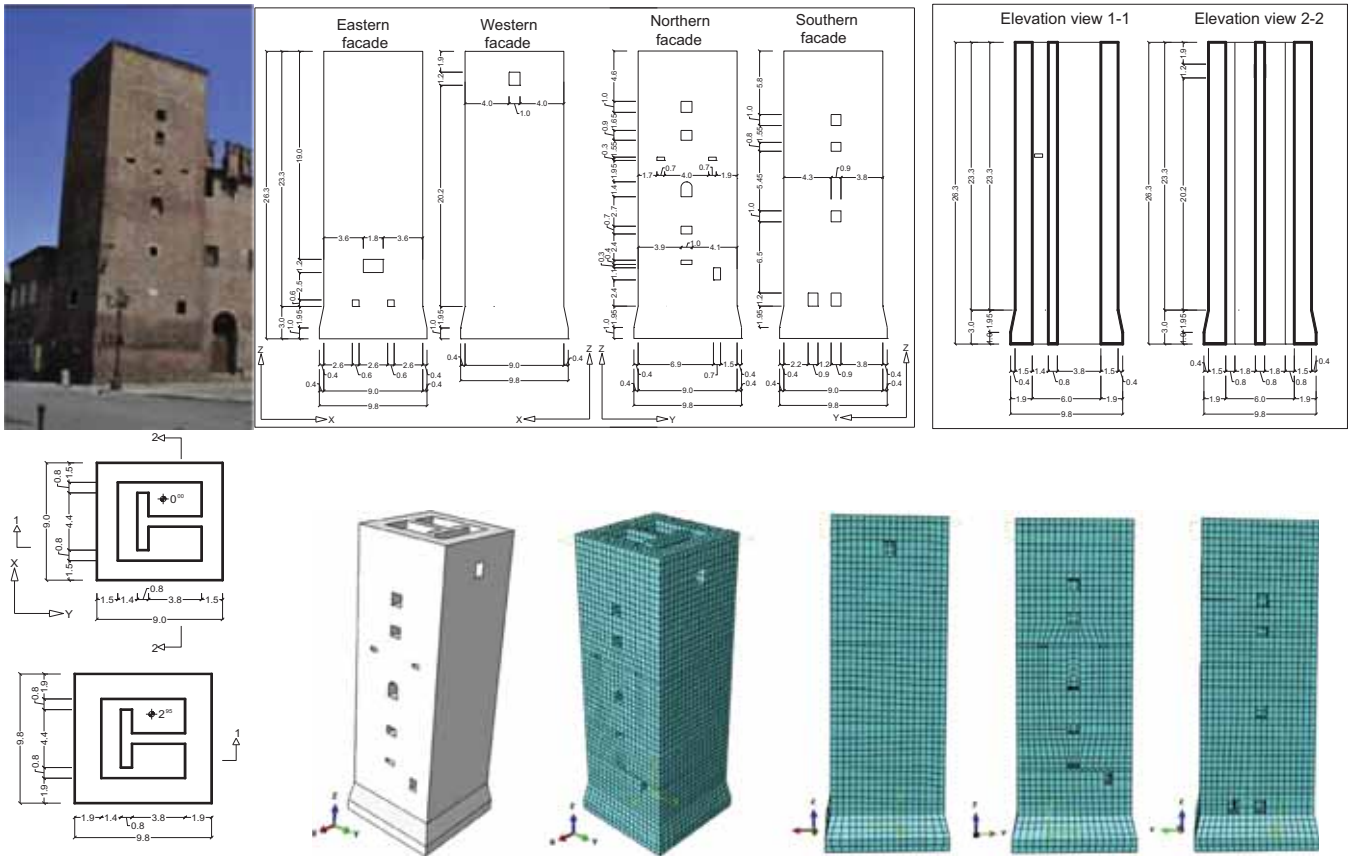

Fig. 5. Tower IV, maistra tower of Praetorian palace.

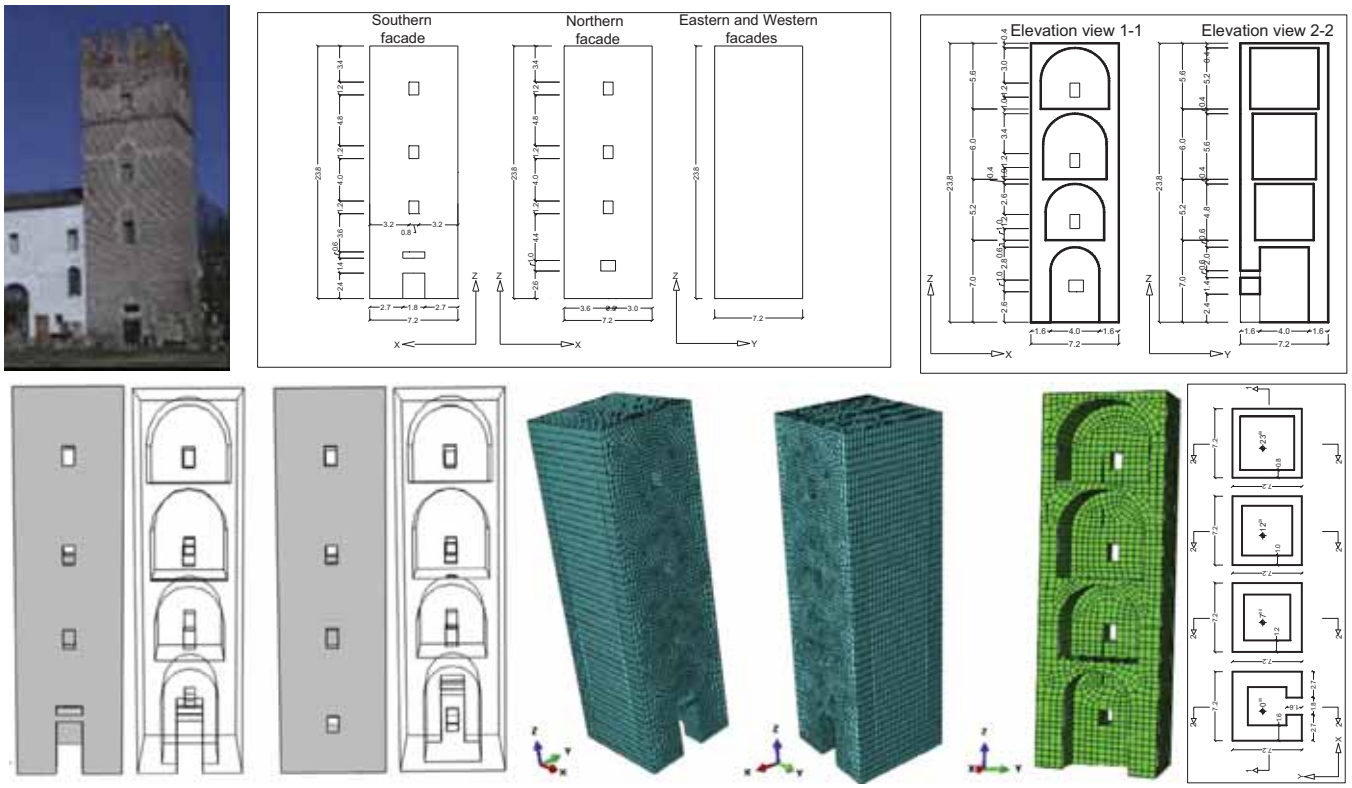

Fig. 6. Tower V, tower of Treves castle.

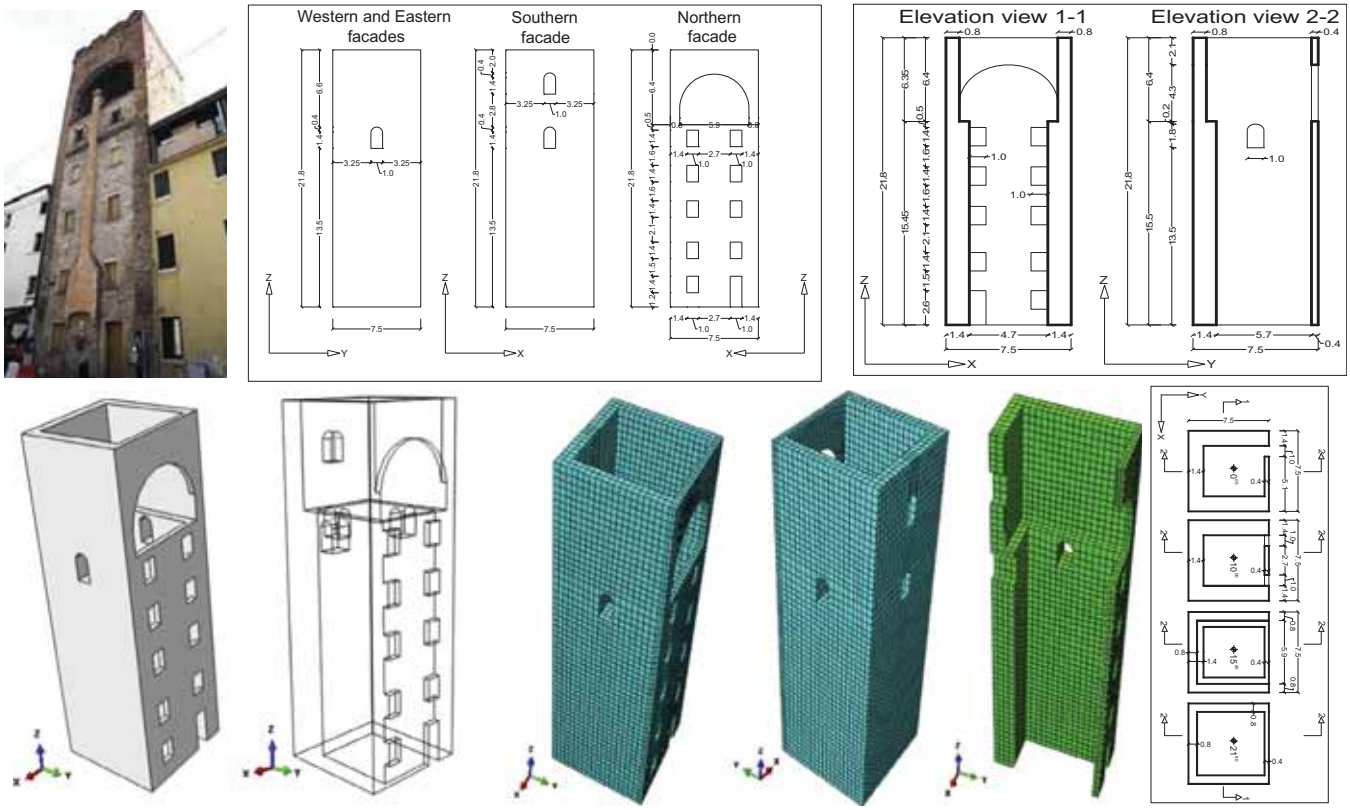

Fig. 7. Tower VI, Pighin tower.

western and eastern prospects, there was an arch that was buffered long time ago. The northern prospect, from the ground floor to the third, was characterized by the presence of a window with a round arch at its top, which was modified later and now the windows have a square shape. There are stringcourse marks below the ceiling of the third floor. All the prospects are decorated with merlon elements on the top of the tower. Due to its historical and architectural importance, an urgent restoration of both internal and external parts is needed, which would bring back its original situation.

The area of Arquà Polesine exhibits medium/low seismicity. Historical records show that the strongest earthquake occurred in a radius of 30 km from the city dates back to 1234 (Ferrara earthquake, about 22 km far from the town) with magnitude $M = 5.17$, while the latest and strongest one occurred on May 20th 2012 with magnitude $M = 5.1$. During the last 5 years (2009–2014), 85 earthquakes were recorded within the given radius, all of them with a magnitude between 2 and 5.1.

2.6. Pighin tower (Tower VI)

Tower VI, see Fig. 7, is a defence tower located in Rovigo in Veneto region. Since the tower was built (12th century) as a Medieval defence structure, it was totally opened towards the city. With the evolution of the military technology, the tower lost its strategic importance and around 1775 the missing wall was filled when the structure became a part of a residential building. Pighin tower, whose real name is "St. Augustine door", is structurally rather simple. The height is equal to 21.8 m and the slenderness is about 2.9. It is internally subdivided into six floors. Originally, it had wooded slabs, connected by ladders. Each of the floors has a square plan and consists of a single compartment. Three walls have a thickness of 140 cm for the first five storeys and a thickness of 80 cm for the last storey, whereas the thickness of the wall that was built later is equal to 40 cm for the whole height of the structure. The eastern and western facades are almost identical; there is also a quite unusual chimney on the northern façade, added when the tower became a residential building. The structure that can be seen today is almost the original one, dating back to the eighteenth century. A recent restoration was done in the year 1983, mainly constituted by light re-stitching of the mortar joints.

Historical records show that the strongest earthquake, in a radius of 30 km from the city, occurred in 1234 in Ferrara (29.42 km far from Rovigo) with a magnitude $M = 5.17$, while the latest and strongest one occurred on May 20th 2012 with magnitude $M = 4$. During the last 5 years (2009–2014), more than 20 earthquakes were recorded within the given radius, all of them with a magnitude between 2 and 4.

2.7. Bell tower of San Sisto II church (Tower VII)

Tower VII, see Fig. 8, is a bell tower belonging to the church of San Sisto II in Palidano, a small town between the cities of Modena and Mantua in Lombardia region. The structure is built in Romanesque style and exhibits a height of 22.6 m and the slenderness is about 4.8. It is internally subdivided into six storeys, with wooden floors connected by a wooden staircase. All of the floors are approximately square in plan (4.7/5.1 m) and consist of a unique space, which is partly occupied by the staircase. The tower exhibits a marked inclination with an out-of-verticality reaching 0.6 m at a height of 17 m. The thickness of the four perimeter walls is constant along the height and equal to 1.4 m for one of the walls and 0.8 m for the others. The bell is framed by a belfry with large arched windows. The rest of the openings are very small and located in the western and eastern façades only.

The area of Palidano is classified as a low/medium seismicity region. However, historical records report that the strongest earthquake, in a radius of 30 km from the city, occurred on 22 February

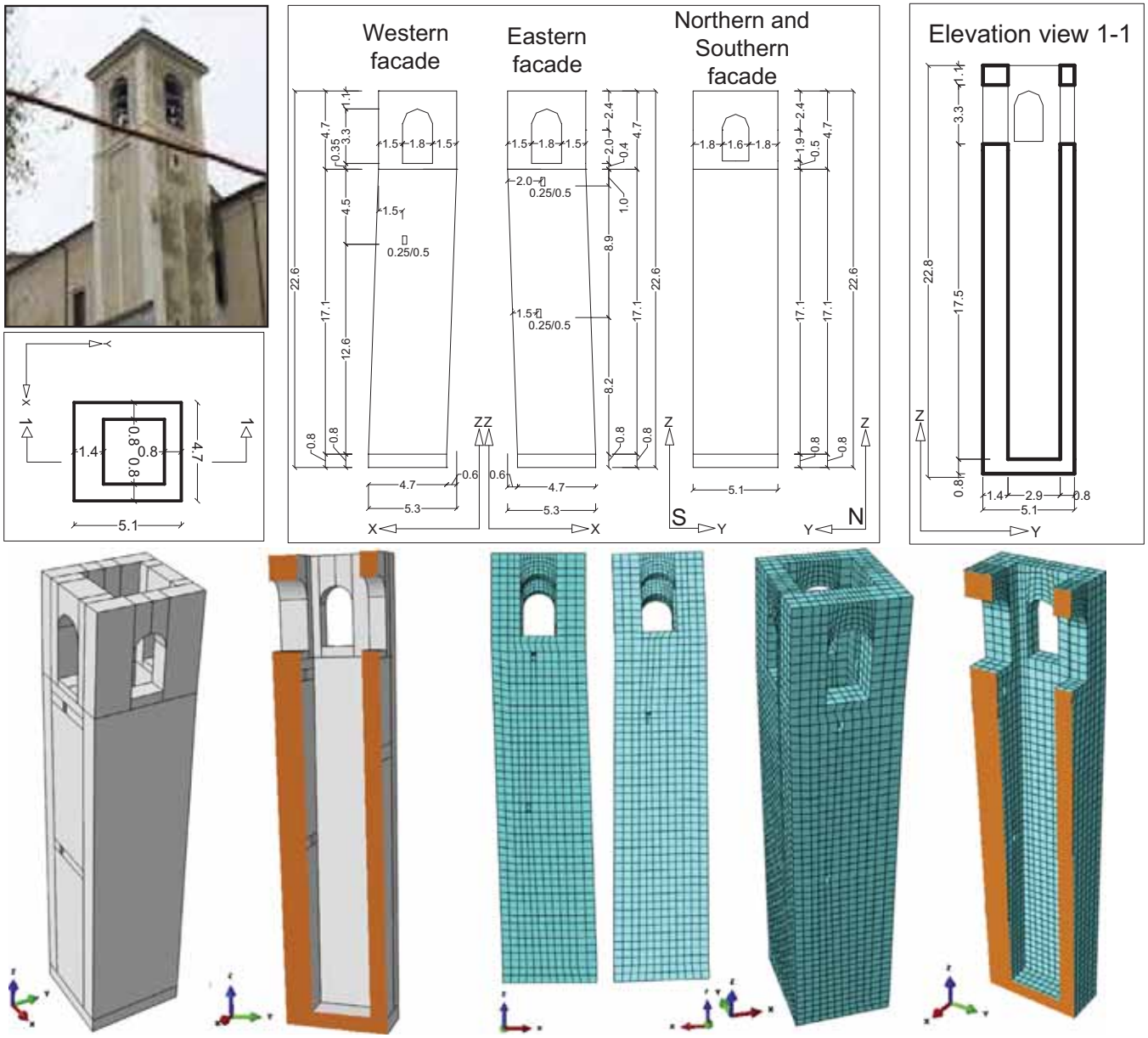

Fig. 8. Tower VII, bell tower of San Sisto II church.

1346 at Concordia sulla Secchia (19.8 km far from Palidano) with a magnitude $M = 5.81$, During the last 5 years (2009–2014), 925 earthquakes were recorded within the given radius, all of them with a magnitude between 2 and 5.8. The recent 2012 Emilia-Romagna seismic sequence resulted into a severe damage of both the church and the bell tower, which is now subjected to a comprehensive structural rehabilitation by means of the introduction of pre-tensioned tie rods at the floor levels of the perimeter walls.

2.8. Morosini tower (Tower VIII)

Tower VIII, see Fig. 9, is located in Lusia, a small town in the province of Rovigo in Veneto region. In the past, the tower belonged to a magnificent complex known as Morosini Villa. Now, it is the only evidence of such a complex, that was completely destroyed during the second world war. The tower presents a height of 22.5 m and the slenderness is about 3.2. It is internally subdivided into four storeys (one of them is a basement), connected by a spiral wooden staircase. Every floor consists of three rooms – one of them occupied by the staircase and the other two having magnificent vault ceilings. The walls have a thickness of 40–80 cm. Externally, the corners between the walls, the windows and the doors are adorned by a decorative ashlar. The stone blocks are apparently of good quality and well-preserved. The traces of the junction of the tower with the surrounding buildings can be still seen (with the main building through the west wall and with a small building through the south wall) – in particular, the punctures due to the intersection of the beams and the strips. The tower is crowned by battlements. In 1998 it was object of a restoration intervention, still not finished for budget limitations. At present, new signs of deterioration can be seen, so far limited, but showing that there is the need to take some rehabilitation measures.

Historical records show that the strongest earthquake near Lusia, in a radius of 30 km, dates back to the 1234 Ferrara earthquake (29.6 km far from the town) with magnitude $M = 5.17$, while the latest and strongest one occurred on 20 February 1956 with a

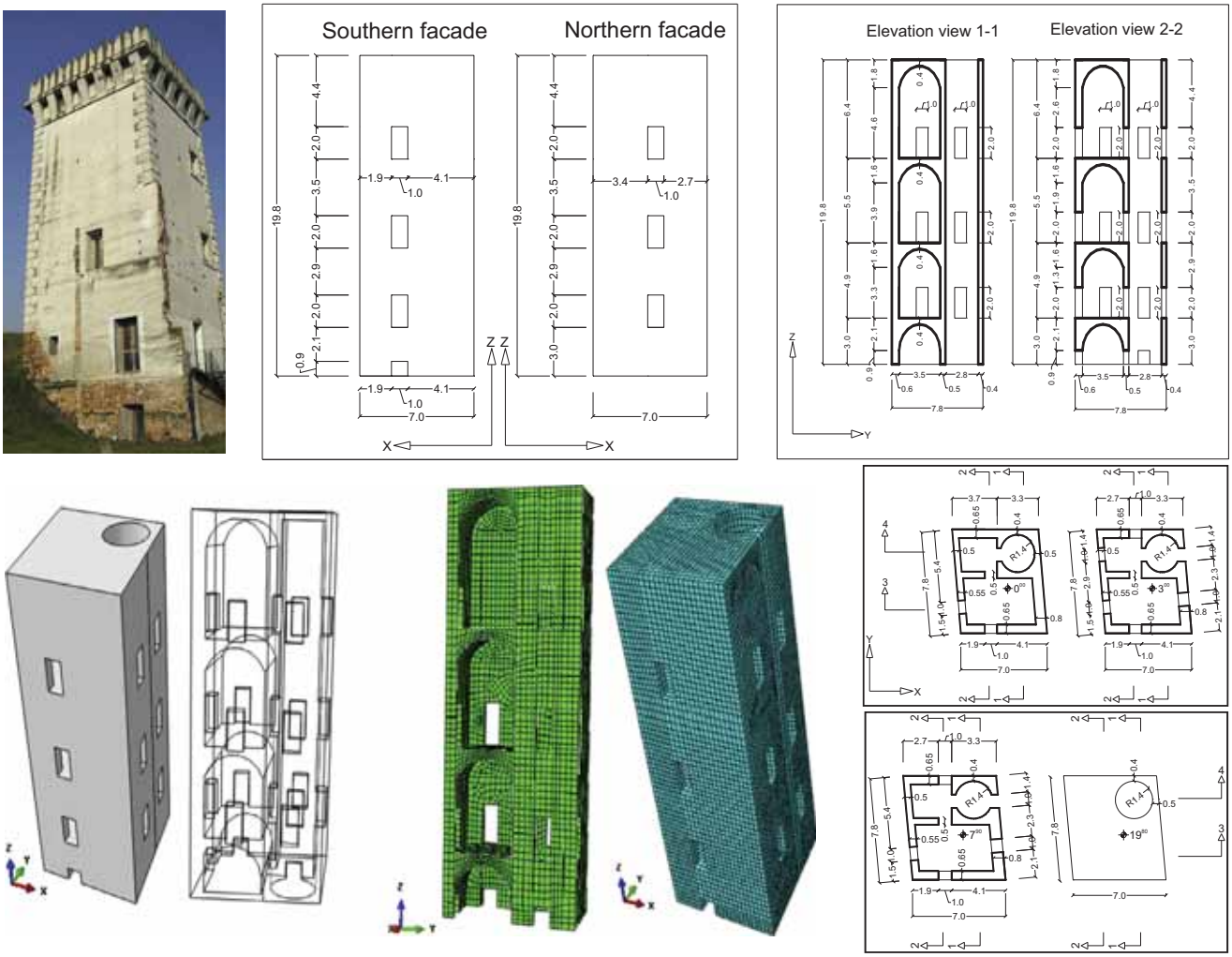

Fig. 9. Tower VIII, Morosini tower.

magnitude $M = 4.98$. During the last 5 years (2009–2014) almost 30 earthquakes were recorded within the given radius, all of them with a magnitude between 2 and 3.

3. The material model adopted

Three-dimensional finite element models of the different towers are created and non-linear static analyses are conducted by means of the computer code ABAQUS [25] assuming for masonry a Concrete Damage Plasticity (CDP) material model, which is available within the software and within many other FE codes. Although a CDP approach is conceived for isotropic fragile materials like concrete, it has been widely shown that its basic constitutive law can be also adapted to masonry, see for e.g. [7–9,15]. It is worth noting, indeed, that experimental results reported by Page on regular masonry wallets [26] and successive numerical models [27] show that such a material exhibits a moderate orthotropy ratio (around 1.2) under biaxial stress states in the compression–compression region. Obviously, such feature cannot be taken into account when an isotropic model, like the present one, is utilized. However, it is commonly accepted in the literature the utilization of isotropic models (like concrete smeared crack approach available in both Ansys and Adina), after an adaptation of the parameters, to fit an average behavior between vertical and horizontal compression. A suitable model should also take into account the ratio between the ultimate compression strength in biaxial stress states and in uniaxial conditions. CDP model allows analyzing materials with different strength in tension and compression, assuming distinct damage parameters. Compressive crushing is also described by means of the introduction of plastic deformation with a parabolic softening law.

In tension, see Fig. 11, the stress–strain response follows a linear elastic relationship until the peak stress σ_{t0} is reached. Then, micro-cracks start to propagate in the material, a phenomenon that is macroscopically represented by softening in the stress–strain relationship. Under axial compression, the response is linear up to the value of the yield stress σ_{c0}. After the yield stress, the response is typically characterized by hardening, which anticipates compression crushing, represented by a softening branch beyond the peak stress σ_{cu}.

The damage variables in tension d_t and in compression d_c are defined by means of the following standard relationships:

$$\sigma_t = (1 - d_t)E_0(\varepsilon_t - \varepsilon_t^{pl})$$
$$\sigma_c = (1 - d_c)E_0(\varepsilon_c - \varepsilon_c^{pl}) \quad (1)$$

where $\sigma_t(\sigma_c)$ is the mono-axial tensile (compressive) stress, E_0 is the initial elastic modulus, ε_t (ε_c) is the total strain in tension (compression), $\varepsilon_t^{pl}(\varepsilon_c^{pl})$ is the equivalent plastic strain in tension (compression). In the present study, damage is assumed active in tension only, since the tensile strength of the material is very low, especially in comparison with the compressive one. When strain reaches a critical value, the material elastic modulus degrades in the unloading phase to $E < E_0$. In particular, in the numerical simulations a reduction equal to 5% of the Young modulus with respect to the initial value is assumed for a plastic deformation equal to 0.003.

The strength domain is a standard Drucker–Prager surface modified with a so-called *Kc* parameter, see Fig. 12, representing the ratio between the distance from the hydrostatic axis of the maximum compression and tension, respectively. As suggested by the user's guide, it is kept equal to 0.667 in all computations. The tension corner is regularized with a correction parameter referring to eccentricity, see Fig. 13. The user's guide suggests a default value of 0.1. A value of 10° is adopted for the dilatation angle for the inelastic deformation in the non-linear range, which is in agreement with the data suggested in [28]. The ratio between the bi-axial (f_{bo}) and mono-axial (f_{co}) compression strength has been kept equal to 1.16 as suggested in the literature, [26], [27,28], for concrete (masonry behavior found to be similar). The values of the various inelastic parameters adopted for the analyses are defined in Table 1.

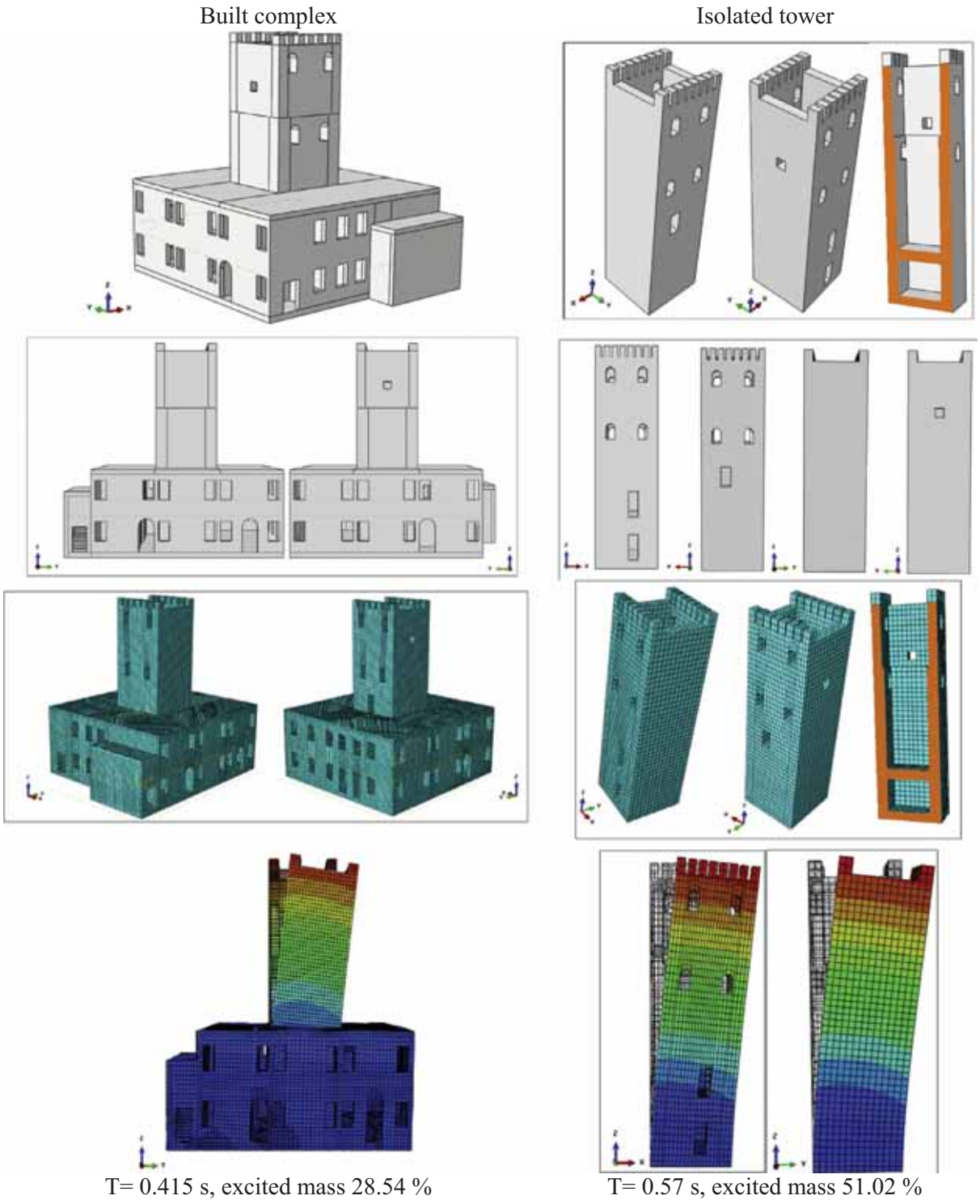

Fig. 10. Tower I: numerical models of the built complex and isolated tower and comparison of the fundamental mode.

Whilst the utilization of the CDP model is probably more in agreement with the actual behavior of masonry, its utilization requires experienced users [29] and huge computational time for both pushover [30] and non-linear dynamic [31] analyses, especially when 3D FE models with many elements are used. The issue of mechanical properties to adopt for the constituent materials is very tricky. It is common opinion, indeed, that the major damages registered in historical buildings, such as towers, castles and churches, are a consequence of very poor mechanical properties of joints, whereas clay bricks exhibit a quite high strength in such Italian region. In the absence of ad-hoc experimental campaigns performed on the case studies at hand, it is necessary to refer to what is stated by Italian Code for existing masonry buildings. As a matter of fact, masonry is a material which exhibits distinct directional properties due to the mortar joints, acting as planes of weakness. Considering the well-known limitation of the use of both micro-modeling and homogenization at large scale, isotropic macro-models are adopted for masonry. The reason for adopting an isotropic material stands in the impossibility to evaluate many parameters necessary for anisotropic materials in the inelastic range, in the absence of ad-hoc experimental characterizations. Finally, it is worth noting that commercial codes rarely put at disposal to users anisotropic mechanical models suitable to describe masonry with a regular texture in the non-linear range.

According to Italian code NTC 2008 [1] and subsequent Explicative Notes [2], the mechanical properties assumed for masonry material depend on the so-called knowledge level LC, which is related to the so-called Confidence Factor FC. There

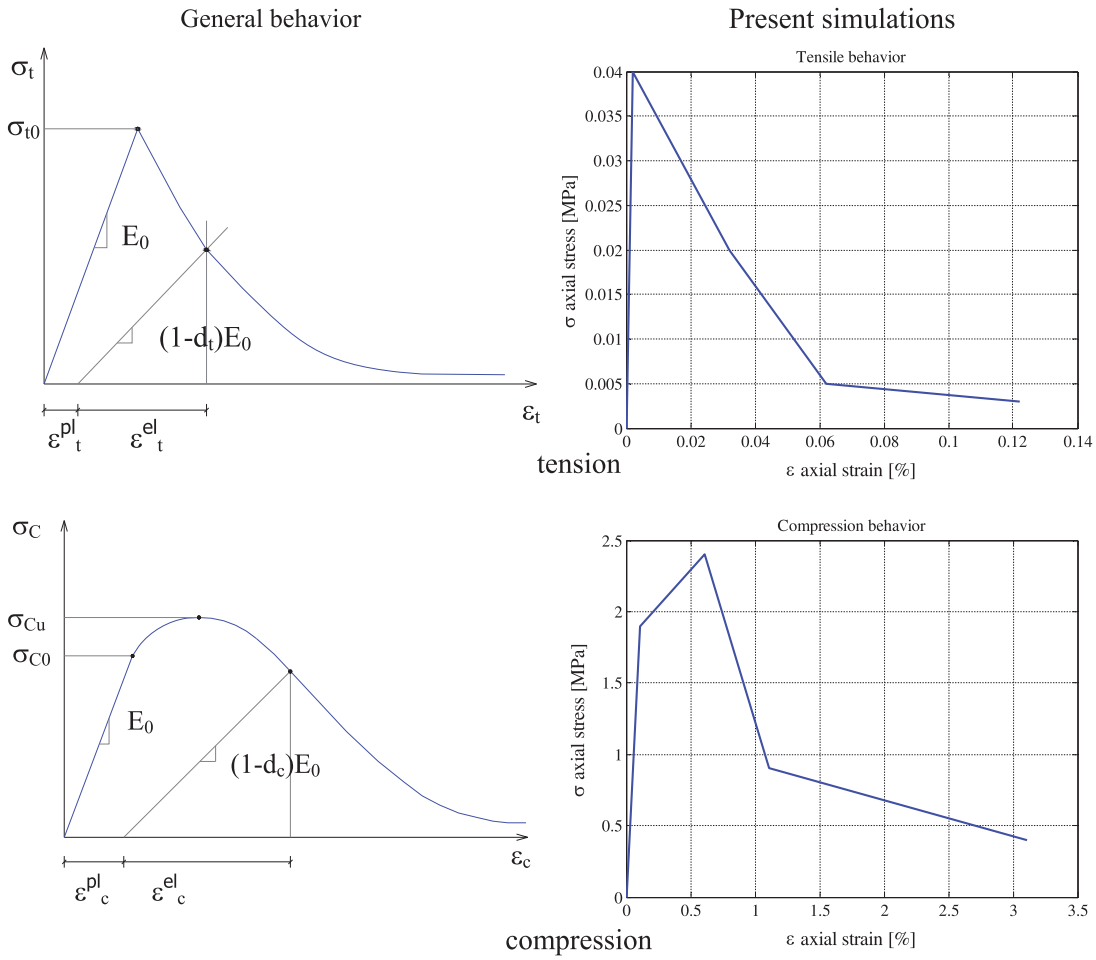

Fig. 11. Constitutive law in tension and compression adopted for masonry.

are three LCs, labeled from 1 to 3, related to the knowledge level of the mechanical and geometrical properties of the structure. The knowledge level LC3 is the maximum, whereas LC1 is the minimum. For the cases at hand, a LC1 level is assumed in the absence of specific in situ test results.

As a consequence, the values adopted for cohesion and masonry elastic modulus are taken in agreement with Explicative Notes [2] of the Italian code NTC 2008 [1], assuming a masonry typology constituted by clay bricks with very poor mechanical properties of the joint and quite regular courses. The stress–strain relationships adopted in the ABAQUS model are therefore those depicted in Fig. 11, which (where data are available) are in agreement with the Italian code requirements.

4. Eigen-frequency analysis

In order to obtain a preliminary assessment of the dynamic behavior of the towers under study, an eigen-frequency analysis is performed on the three-dimensional FE models. It can be noted that the ability of such a conventional analysis to represent the actual behavior of the structure is limited because the intrinsic behavior of masonry structures is known to be strongly non-linear during seismic excitation. In any case, preliminary standard eigen-frequency analyses may provide some basic information about the dynamic behavior of the different towers and allow identifying – among other results and in the framework of linear elasticity – the vibration modes characterized by a high participating mass as well as the corresponding periods to compare with accelerations provided by code response spectra. It can be observed that the eigen-frequency analysis is useful for the non-linear static procedure adopted in this study. Italian code requires the knowledge of the normalized fundamental mode displacement vector in order to reduce the structure to a single degree of freedom (SDOF) system. Moreover, the knowledge of eigen-values, eigen-modes and the corresponding excited mass is required for the determination of the horizontal load distribution in the non-linear static pushover analyses.

In general, it is found that, apart from some specific cases where significant structural irregularities can modify/reduce the participating mass, the behavior of all towers is quite well approximated by a cantilever beam schematization with a uniform distribution of mass and stiffness: the first two modes are flexural and the third mode is torsional.

Fig. 14 shows the modal deformed shapes corresponding to the first main modes of the towers under study. The distribution of the main modes (with an excited mass higher than 5%) in the *X* and *Y* directions with reference to the response spectrum provided by Eurocode 8 with soil type C is presented in Fig. 15, where dashed vertical lines define the upper and lower periods bracketing the horizontal plateau. A vibration mode with the corresponding period within such an interval is associated with the highest seismic acceleration (at least assuming an elastic material model) and hence is more likely to occur. Almost systematically, it is found that periods provided by modal analyses present the highest excited mass near the plateau of the code response spectrum. Despite the clear limitations of the approach proposed mainly linked to the assumption of an elastic behavior, it can be affirmed that eigen-frequency analyses could be useful for practitioners, indicating that a flexural failure with formation of a plastic hinge near the base is more likely to occur in the case of earthquake.

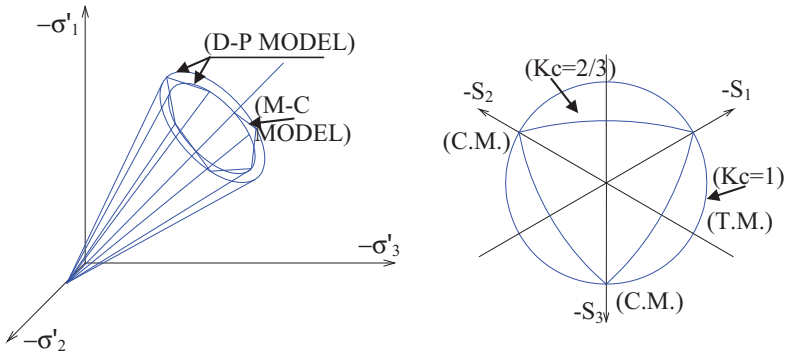

Fig. 12. 3D strength domain adopted in ABAQUS for the CDP model and meaning of *Kc* parameter. D–P: Drucker Prager strength criterion. M–C: Mohr–Coulomb strength criterion. C.M.: compressive meridian. T.M.: tensile meridian.

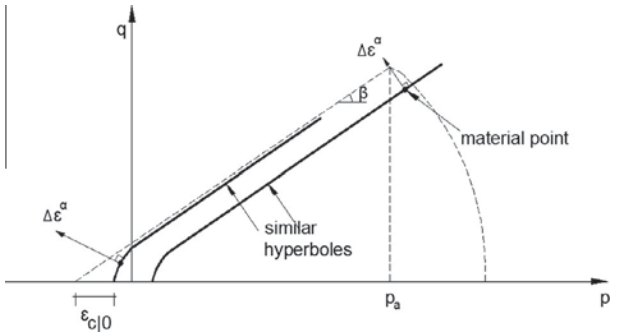

Fig. 13. Smoothed Druker-Prager failure criterion adopted in the simulations, *p*–*q* plane.

Table 1
Mechanical properties adopted for the analyses.

Type	Parameter	Value
	Poisson's Ratio	0.2
	Dilatation angle	10°
Concrete damaged plasticity	Eccentricity	0.1
	σ_{b0}/σ_{c0}	1.16
	K	0.666
	Viscosity Parameter	0.002

4.1. Tower I

The dynamic behavior of the tower is similar in both the directions because of the square cross-section of the tower. It is affected mainly by the reduction of the walls thickness in the upper part and by the presence of some openings in the walls in the *X* direction. The first period of the tower is equal to 0.57 s and it is related to a modal shape mainly translational in the *X* direction with a participating mass ratio of 52% and a small component in the *Y* direction with a participating mass ratio of 8%. The second period of the tower is equal to 0.56 s and it is related to a modal shape mainly translational in the *Y* direction with a participating mass ratio of 50% and a small component in the *X* direction with a participating mass ratio of 8%. The third mode with a period of 0.22 s is dominantly torsional. The first six modes correspond to a total participating mass ratio of 81% and 80% in the *X* and *Y* directions, respectively.

4.2. Tower II

The first two bending modes of the tower have close frequency values because of the nearly square symmetric shape of the tower. Minor differences depend mainly on some small openings. The first and second eigen-frequencies of the tower are related to modal shapes completely translational in the *Y* and *X* directions, respectively, with a participating mass ratio of 52%. The periods associated with the first two modes are 0.89 s and 0.87 s. The third and fourth eigen-frequencies evidence a translational shape in the *Y* and *X* directions, with a participating mass ratio of 23% and 21%, respectively. The fifth mode presents a predominant torsional component. The first six modes correspond to a total participating mass ratio of 75% and 74% in the *X* and *Y* directions, respectively. The higher modes are characterized by low participating mass ratios and are local modes involving mainly the upper part of the tower.

4.3. Tower III

The large openings at the base of the tower significantly affect the dynamic behavior of the tower. The first vibration mode of the tower is essentially characterized by a motion along the *Y* direction, with a period of 0.6 s and a participating mass ratio of 78%. The second vibration mode of the tower is completely translational in the *X* direction, with a period of 0.55 s and a participating mass ratio of 61%. The fifth mode is torsional with a corresponding period of 0.30 s. The first eight modes correspond to a total participating mass ratio of 77% and 93% in the *X* and *Y* directions, respectively. The higher modes are characterized by low participating mass ratios and are local modes involving mainly the upper part of the tower.

4.4. Tower IV

The tower presents a square cross-section with a small variation of the wall thickness along the height. The dynamic behavior of the tower is partially influenced by the arrangement of the T-shaped inner walls. The first eigen-frequency of the tower is related to a modal shape completely translational in the *X* direction, with a participating mass ratio of 59%. The second eigen-frequency of the tower is related to a modal shape completely translational in the *Y* direction, with a participating mass ratio of 61%. The third mode presents a predominant torsional component. The periods associated with the first three modes are 0.73 s, 0.7 s and 0.48 s. The first eight modes correspond to a total participating mass ratio of 81% and 82% in the *X* and *Y* directions, respectively.

4.5. Tower V

The dynamic behavior of the tower is affected mainly by the presence of internal vaults and some small openings. The first eigen-frequency of the tower is related to a modal shape completely translational in the *X* direction, with a period of 0.68 s

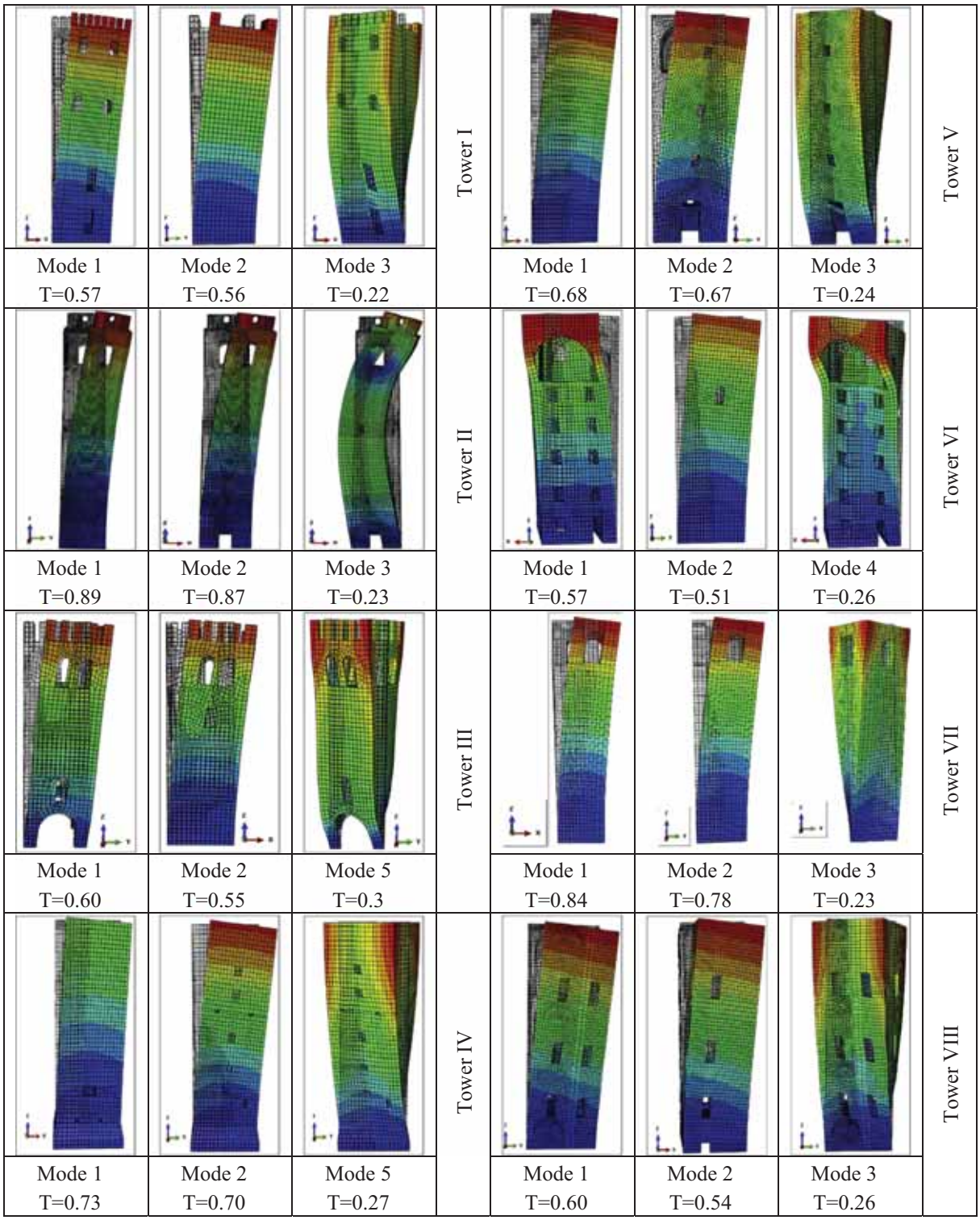

Fig. 14. Elevation views of the deformed shapes of the first main modes and corresponding periods (in seconds).

and a participating mass ratio of 59%. The second eigen-frequency of the tower is related to a modal shape completely translational in the *Y* direction, with a period of 0.67 s and a participating mass ratio of 60%. The third mode is dominantly torsional with a corresponding period of 0.24 s. The first five modes correspond to a total participating mass ratio of 82% and 83% in the *X* and *Y* directions, respectively.

4.6. Tower VI

Tower VI is not symmetrical in plan because one of the perimeter walls in the *X* direction presents a smaller thickness than the other walls. Moreover, the same wall is characterized by multiple openings along the height and a large arch, which significantly reduces the structural stiffness, is present on the top. The first

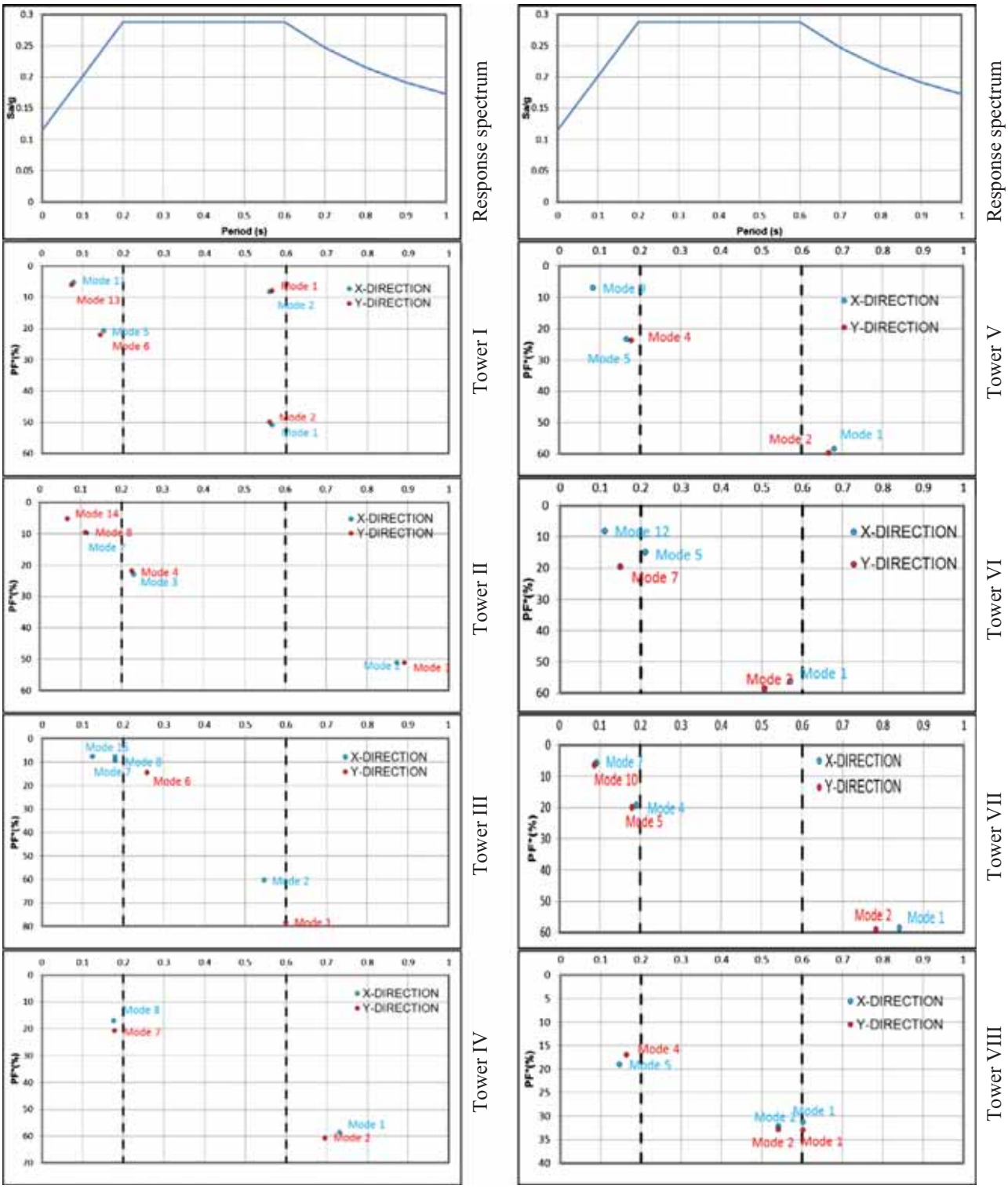

Fig. 15. Response spectrum and distribution of the main modes with effective modal mass greater than 5% of the total mass in the *X* and *Y* directions.

mode evidences a torsional shape, with a prevalent translational component in the *X* direction, as evidenced by the participating mass ratio of 57%. A more pronounced deformation is observed in the upper part of the tower, caused by the presence of the large opening. The second eigen-frequency of the tower is related to a modal shape completely translational in the *Y* direction, with a participating mass ratio of 59%. The periods associated with the first two modes are 0.57 s and 0.51 s. The third mode is a local mode, which involves the upper part of the tower near the large opening, with negligible participating mass ratio. The fourth mode exhibits a predominant torsional component. The first seven modes correspond to a total participating mass ratio of 75% and 78% in the *X* and *Y* directions, respectively. The presence of local modes, involving mainly the region near the large opening, clearly highlights the critical situation of the upper part of the tower, pointing out the need to carry out structural interventions.

4.7. Tower VII

The tower exhibits a quite relevant inclination and is not symmetrical in plan because the thickness of one wall is much larger than the other walls. Moreover the dynamic behavior of the tower is affected by the presence of large openings at the top. The first eigen-frequency of the tower is related to a modal shape translational in the *X* direction, with a period of 0.84 s and a participating mass ratio of 59%. A slight torsional component is also observed. The second eigen-frequency of the tower is related to a modal shape translational in the *Y* direction, with a period of 0.78 s and a participating mass ratio of 60%. The third mode is a torsional mode with a period of 0.23 s. It is possible to observe that the upper part of the structure has a flexible behavior due to the presence of the large openings. The first six modes correspond to a total participating mass ratio of 78% and 79% in the *X* and *Y* directions, respectively. The higher modes are characterized by low participating mass ratios and are local modes involving mainly the upper part of the tower.

4.8. Tower VIII

The tower presents some irregularities in plan and the first two modes involve a motion of the tower along an axis oblique to the main axes. The first mode is translational with a participating mass ratio of about 31% and 33% in the *X* and *Y* directions, respectively. The second mode is translational with a participating mass ratio of about 32% and 33% in the *X* and *Y* directions, respectively. The third mode presents a prevalent torsional component. The periods associated with the first three modes are 0.6 s, 0.54 s and 0.26 s. The first five modes correspond to a total participating mass ratio of 84% and 83% in the *X* and *Y* directions, respectively.

As usually occurs for towers, it is worth noting that the largest participating mass ratio in the two orthogonal directions corresponds to the first two modes. The behavior along the *X* and *Y* directions is similar due to the nearly square cross-section of the towers under consideration. Small differences depend mainly on some geometric irregularities in plan and elevation, such as presence of openings, variation of wall thickness and internal vaults distributions. Moreover, it can be noted that the periods of the main modes of the majority of the towers fall in or near the constant branch of the response spectrum (soil type C) providing the maximum value of spectral acceleration. The fundamental frequencies obtained can be compared with the dominant frequencies characterizing the earthquakes expected at the site in order to estimate the amplification effects. In some cases, the eigen-frequency analysis highlights the presence of local modes involving mainly the upper part of the towers where large openings are present. This preliminary analysis may be useful for a first rough evaluation of the weaknesses of the structure in order to develop suitable interventions of consolidation to reduce the seismic vulnerability of the towers.

5. Simplified assessment procedure based on non-linear static analysis

A simplified displacement-based procedure using non-linear static pushover analyses [30] is adopted for the seismic verification of the global performance of the eight towers. According to Italian code [1,2], when dealing with pushover analyses, the response of the structure should be investigated along the geometrical orthogonal axes *X* and *Y*, in both the positive and negative directions. Italian code also prescribes the evaluation of the load carrying capacity by means of two vertical configurations of lateral forces: a first distribution of forces derived by the assumption of a linear variation of acceleration along the height (G1) and a second distribution with uniform acceleration (G2). For the towers under consideration, distribution G1 always provides collapse accelerations lower than those provided by distribution G2, therefore the reduction of the structure to a SDOF (single degree of freedom) system is done with reference to distribution G1. In the case of different structural behavior along the positive and negative directions (e.g. $+X$ and $-X$, or $+Y$ and $-Y$), the more conservative results are considered. Distributions G1 and G2 are automatically applied to ABAQUS meshes by means of user defined "body forces" functions. The base shear is plotted against the displacement of a control point placed at the top of the tower, having experienced a quite global flexural/shear collapse mode during non-linear static analyses.

The pushover curve is scaled by means of the transformation factor $\Gamma = \frac{\sum m_i \Phi_i}{\sum m_i \Phi_i^2}$, where Φ_i is the ith component of the eigenvector Φ and m_i is the mass of the node i. Assuming as F_b and d_c the actual base shear and the corresponding top displacement of the structure respectively, the scaled values are $F_b^* = F_b/\Gamma$ and $d_c^* = d_c/\Gamma$. The peak base shear, denoted as F_{bu}, is given by $F_{bu}^* = F_{bu}/\Gamma$.

The seismic demand is defined in the form of an elastic acceleration response spectrum S_{ae}(T), where the spectral accelerations are defined as a function of the natural period T of the structure. In this study, the seismic demand is computed with reference to the response spectrum provided by Eurocode 8, where the constant spectral acceleration branch is estimated as $S_e = 2.5 a_g S \eta$: a_g is the design ground acceleration on soil type A, S is the soil factor and η is the damping correction factor with a reference value of $\eta = 1$ for 5% viscous damping. Two values of peak ground accelerations $S\,a_g$, equal respectively to 0.1 g and 0.2 g, are considered in this study. A soil type C is assumed for all the towers, considering a soil factor S equal to 1.15. While a distinction case by case should be done on the basis of appropriate investigations to identify the local ground conditions, it is reasonable to assume the same soil for the different towers in order to compare the different responses, as in the present case.

The pushover curve of the equivalent SDOF system ($F_b^* - d_c^*$) is reduced to a bilinear elastic-perfectly plastic force–displacement diagram. The bilinear force–displacement diagram is obtained assuming an area equivalence between the equivalent and the bi-linear system, where the equivalent curve is stopped at a displacement d_u^* corresponding to a base shear equal to 85% of the peak base shear. As usually occurs in complex 3D non-linear analyses, a softening of about 15% is hardly reproducible. The numerical analyses are anyway conducted using an arc length routine to deal with possible softening in the global pushover curve, up to a reasonably large displacement of the control point. As explicitly suggested in Italian Guidelines on Cultural Heritage [3], the utilization of materials without softening (like elastic-perfectly plastic models, an hypothesis which implies by definition to find global pushover curves without any softening) is admitted, both because of the extreme complexity in performing non-linear static analyses with detailed 3D geometries and for the diffused unavailability of materials with softening within commonly used commercial codes. On the other hand, it should be pointed out that, even in the presence of softening as in the present damage-plasticity approach, this is hardly visible in the global pushover curves. As commonly known, ultimate capacity for masonry with low tensile strength is, indeed, trivially linked to vertical dead loads and the global contribution of fracture energy cumulated for cracks forming in tension is reasonably negligible. That's one of the reasons why limit analysis computations are preferable in such cases, as stated in [3,32,33]: they are reliable and require a fraction of the

time needed by standard FEM. In the absence of any clear softening, the key question is therefore to identify the correct displacement of the control node where the numerical analysis should be stopped.

In Italian Guidelines on Cultural Heritage [3], considering the difficulties in the definition of the displacement at the ultimate limit state, it is recommended to evaluate the ratio between the elastic limit base shear and the ultimate base shear of the bilinear system. Such a ratio can't exceed a maximum admissible value, defined on the basis of the ductility and dynamic features of each built typology, and in any case ranging between 3 and 6. Typically the aforementioned procedure is iterative, but requires few time for a robust convergence.

On such a basis, taking the lower bound for the sake of safety, pushover curves depicted in Fig. 16 are obtained, with an indication of the corresponding ultimate displacement evaluated iteratively. Results for only two towers are reported for the sake of conciseness. Tower II has a quite symmetrical behavior along the *X* and *Y* directions, whereas Tower VI, due to the evident irregularity near the top, exhibits very different ultimate capacities along the two geometrical directions. This is confirmed by the deformed shapes at collapse (displacement contour plots), again depicted in Fig. 16, where it is pretty evident the formation of a global failure mechanism for Tower II in both the directions (formation of a flexural hinge near the base, cantilever beam behavior) and the formation of a partial out-of-plane failure in correspondence with the large opening near the top of Tower VI in the *X* direction. Authors experienced a similar behavior for all other cases, i.e. softening is not visible in global pushover curves. The elastic stiffness of the SDOF system is estimated plotting the secant line to the pushover curve obtained from ABAQUS in the point corresponding to a base shear equal to 0.7 times the maximum value, again in agreement with [3].

The yield base shear of the equivalent SDOF system is denoted as F_y^*. In the absence of a clear degradation of the base shear, it is assumed $F_y^* = F_{bu}^*$. The ductility of the bilinear curve of the equivalent SDOF system is defined as the ratio between the ultimate d_u^* and the yield displacement d_y^*. Once known the period T^* of the equivalent SDOF system, Italian code allows estimating the displacement demand $d_{\max}^*$ using the elastic displacement spectrum $S_{de}(T)$. Once known $d_{\max}^*$, it has to be checked if $d_{\max}^* \leqslant d_u^*$.

From the elastic acceleration response spectrum it is possible to derive the elastic acceleration–displacement response spectrum (ADRS) using the following expression:

$$S_{de}(T) = \frac{T^2}{4\pi^2} S_{ae}\ (T) \tag{2}$$

In order to evaluate the inelastic acceleration–displacement response spectrum it is necessary to use the reduction factor R_μ linked to the displacement ductility factor μ_s and defined as follows:

$$R_\mu = \begin{cases} 1 + (\mu_s - 1)\frac{T}{T_C} & T < T_C \\ \mu_s & T \geqslant T_C \end{cases} \tag{3}$$

where T_C is the corner period of the plateau of the acceleration–displacement response spectrum.

Conversely, the ductility factor μ_s is dependent on R_μ as follows:

$$\mu_s = \begin{cases} [R_\mu - 1]\frac{T_C}{T^*} + 1 & T^* < T_C \\ R_\mu & T^* \geqslant T_C \end{cases} \tag{4}$$

where $R_\mu = S_{ae}(T^*)/S_{ay}$ can be determined as the ratio between the acceleration of the SDOF system with unlimited linear behavior and the yield acceleration of the SDOF system with limited strength.

From the elastic acceleration–displacement response spectrum the inelastic acceleration–displacement response spectrum is derived if the following expressions are used:

$$S_a(T) = S_{ae}(T)/R_\mu \tag{5}$$

$$S_d(T) = S_{de}(T)\mu_s/R_\mu$$

Finally, the displacement demand $d_{\max}^*$ can be determined using either the graphical procedure (intersection point of the capacity diagram with the demand spectrum corresponding to the ductility demand μ_s) or the following analytical relationship:

$$d_{\max}^* = \begin{cases} \left[1 + (R_\mu - 1)\frac{T_C}{T^*}\right]\frac{S_{de}(T^*)}{R_\mu} & T^* < T_C \\ S_{de}(T^*) & T^* \geqslant T_C \end{cases} \tag{6}$$

5.1. Numerical results

The non-linear static procedure described in the previous section is applied to the towers under study. The seismic vulnerability of the towers is evaluated by means of a comparison between the displacement capacity and the displacement demand obtained through the pushover analyses, both referring to the same control point. The final results are shown graphically from Figs. 17 to 24 for each tower. In such figures, the elastic and inelastic demand spectra and the capacity diagrams (for equivalent SDOF systems), in the acceleration–displacement format (ADSR), are plotted for each tower for two values of peak ground acceleration (Sa_g = 0.1 g and Sa_g = 0.2 g) along the *X* and *Y* directions (more conservative cases). It is worth mentioning that the graphical constructions of both equivalent bi-linear system and inelastic spectra to find displacement capacity and demand are classic issues fully explained in specialized literature (see e.g. [1,2,30]) and are not reported here for the sake of conciseness. It can be only noted that the period of the equivalent SDOF system T^* (defined as $T^* = 2\pi\sqrt{m^*/k^*}$, where k^* is the SDOF stiffness calculated by drawing a line from the origin to the point of the equivalent capacity curve with a base shear equal to 70% of the maximum value and m^* is the equivalent mass) of all the towers under study is larger than the period T_C = 0.6 s, so the equal displacement rule applies and the inelastic displacement demand is equal to the elastic displacement demand.

Finally, for the sake of clarity, the tensile damage distributions corresponding to two values of peak ground acceleration (Sa_g = 0.1 g and Sa_g = 0.2 g) along the *X* and *Y* directions are presented from Figs. 25–32 for each tower.

Hereafter some considerations on the results obtained for each single tower are reported.

5.1.1. Tower I

The pushover analyses show that smaller yield strength is registered for the capacity curve in the *X* direction. Since the structure is symmetrical in plan, this difference can be explained by the presence of multiple openings on the walls in the *X* direction. The non-linear static procedure shows that the displacement demand (7.95 cm) corresponding to Sa_g = 0.2 g is higher than the displacement capacity (5.05 cm) in the *X* direction. Consequently, the verification of the tower is not satisfied in terms of displacements in the *X* direction, see Fig. 17.

Severe damage propagates vertically and concentrates near the openings along the whole height of the walls in the *X* direction, see Fig. 25. The walls in the *Y* direction are damaged mainly in the lower part when the lateral loads are applied in the same direction.

5.1.2. Tower II

The pushover analyses confirm the results obtained from the eigen-value analysis. The elastic stiffness and the yield strength

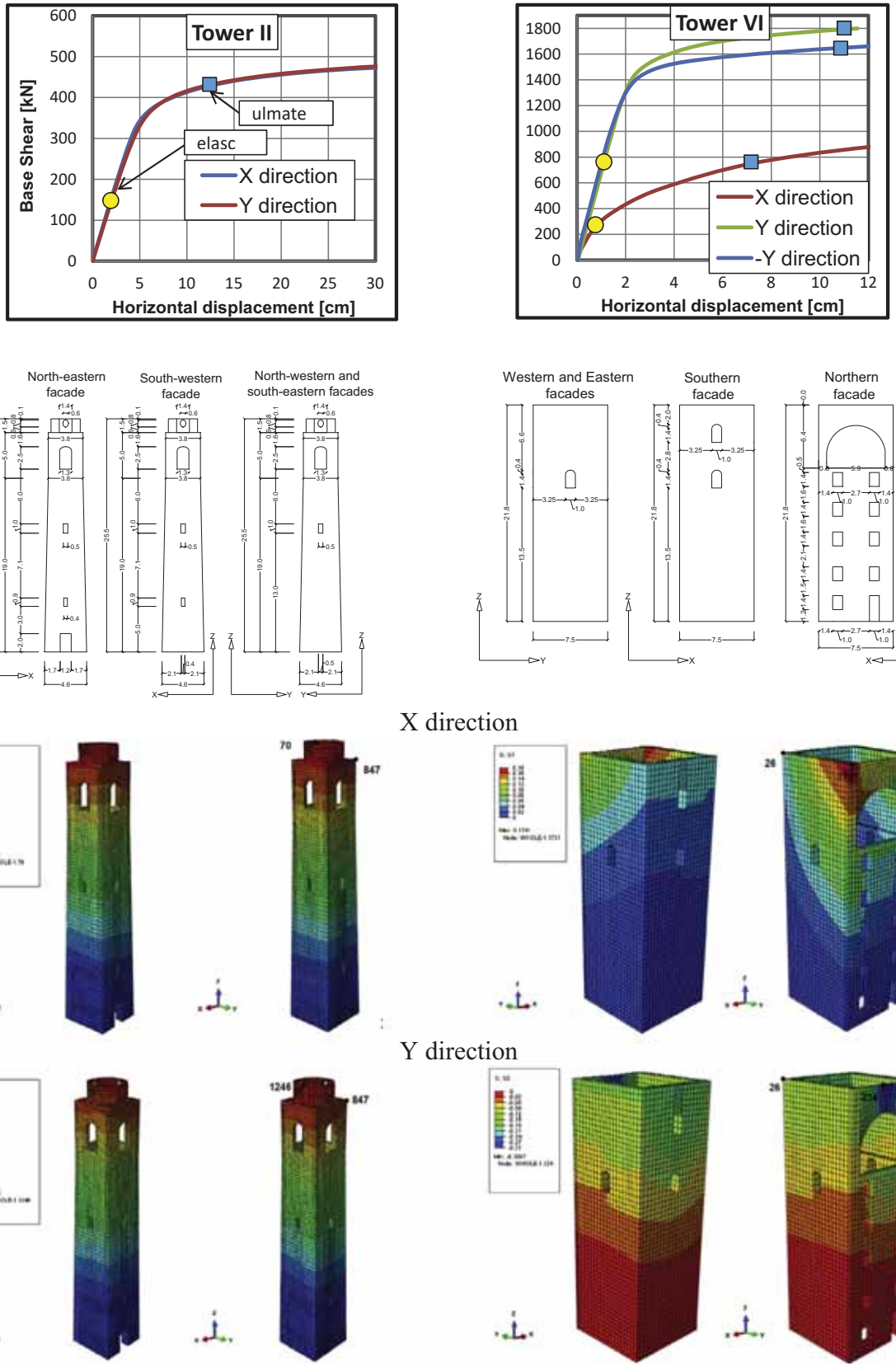

Fig. 16. Tower II and Tower VI: pushover curves obtained for the two orthogonal directions and deformed shapes at collapse with displacement contour plots.

of the system are similar for both the two orthogonal directions. From a geometrical point of view, this tower is symmetrical in plan and the walls present almost the same characteristics in elevation (except the small opening at the base of one wall in the *X* direction). The pushover curves and the seismic demands are very similar in both the directions. The displacement demand (8.6 cm in the

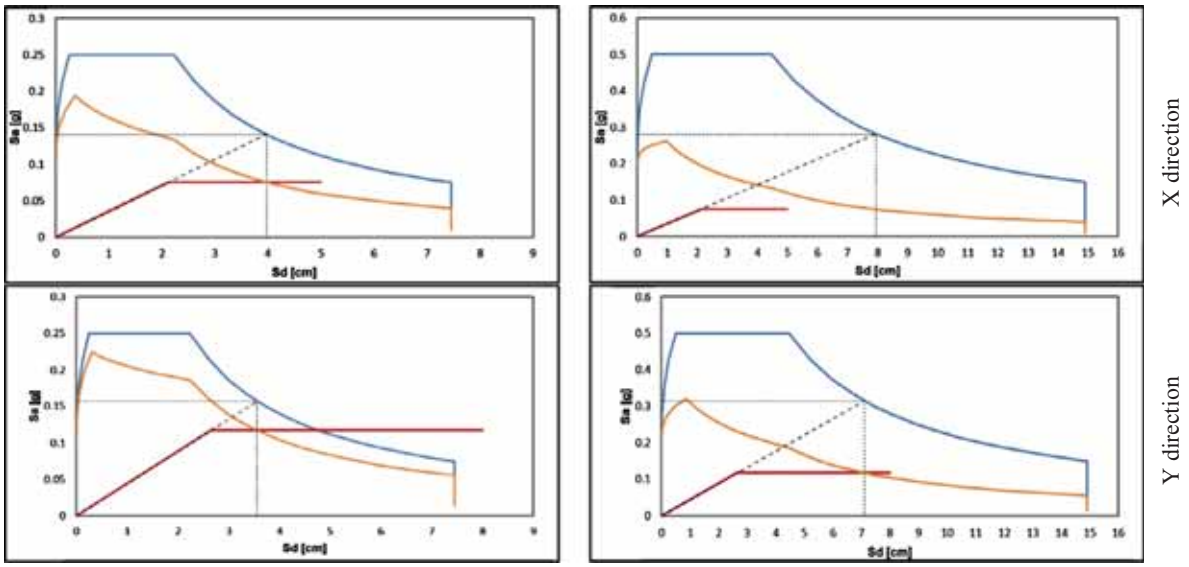

Fig. 17. Tower I: non-linear static procedure in the acceleration–displacement response spectrum plane for different seismic intensity levels (Sa_g = 0.1 g and Sa_g = 0.2 g).

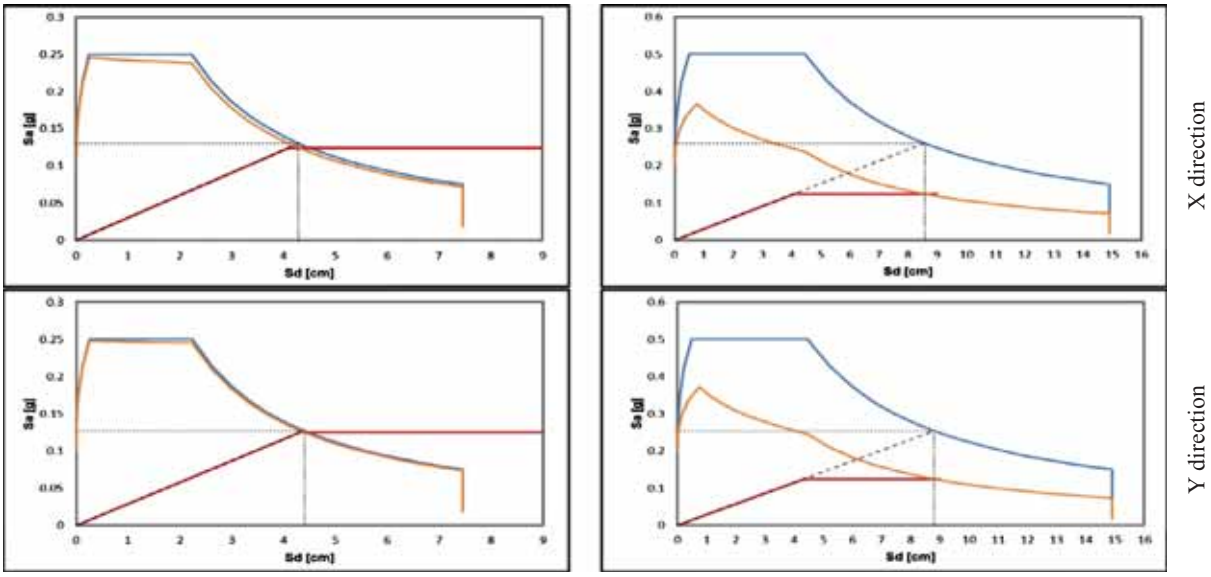

Fig. 18. Tower II: non-linear static procedure in the acceleration–displacement response spectrum plane for different seismic intensity levels (Sa_g = 0.1 g and Sa_g = 0.2 g).

X direction and 8.8 cm in the *Y* direction) corresponding to Sa_g = 0.2 g is lower than the capacity (8.95 cm in the *X* direction and 9 cm in the *Y* direction). The verification of the tower is satisfied in terms of displacements for both the directions, see Fig. 18.

The damage distribution is reported only for the pushover analysis conducted in the *X* direction, because similar damage is observed in the case of the *Y* direction. Damage propagates vertically along the whole height of the tower, see Fig. 26.

5.1.3. Tower III

The pushover analyses indicate different values of both the elastic stiffness and the yield strength of the system for the two orthogonal directions due to the asymmetry of the structure. The two walls in the *Y* direction, up to 4.3 m along the height of the tower, are characterized by two arches, which lead to a decrease of the stiffness and strength in this direction. Above this height, the tower is symmetrical in plan, but not in elevation, since several openings are present in the walls in the *Y* direction.

The displacement demand (7.15 cm in the *X* direction and 7.95 cm in the *Y* direction) corresponding to Sa_g = 0.2 g is higher than the capacity (5.95 cm in the *X* direction and 5.05 cm in the *Y* direction). The verification of the tower is not satisfied in terms of displacements for both the directions, see Fig. 19.

Widespread damage, with the probable occurrence of an active failure mechanism, is registered in the upper part of the walls in the *Y* direction mainly in the case of application of lateral loads in the same direction, see Fig. 27. Damage is evident immediately over the two arches and near the openings at the base.

5.1.4. Tower IV

The pushover analyses confirm the results obtained from the eigen-value analysis. The elastic stiffness and the yield strength of the system are similar for both the orthogonal directions. The structure is symmetrical in plan along the height with respect to the external walls. A small asymmetry is introduced by the

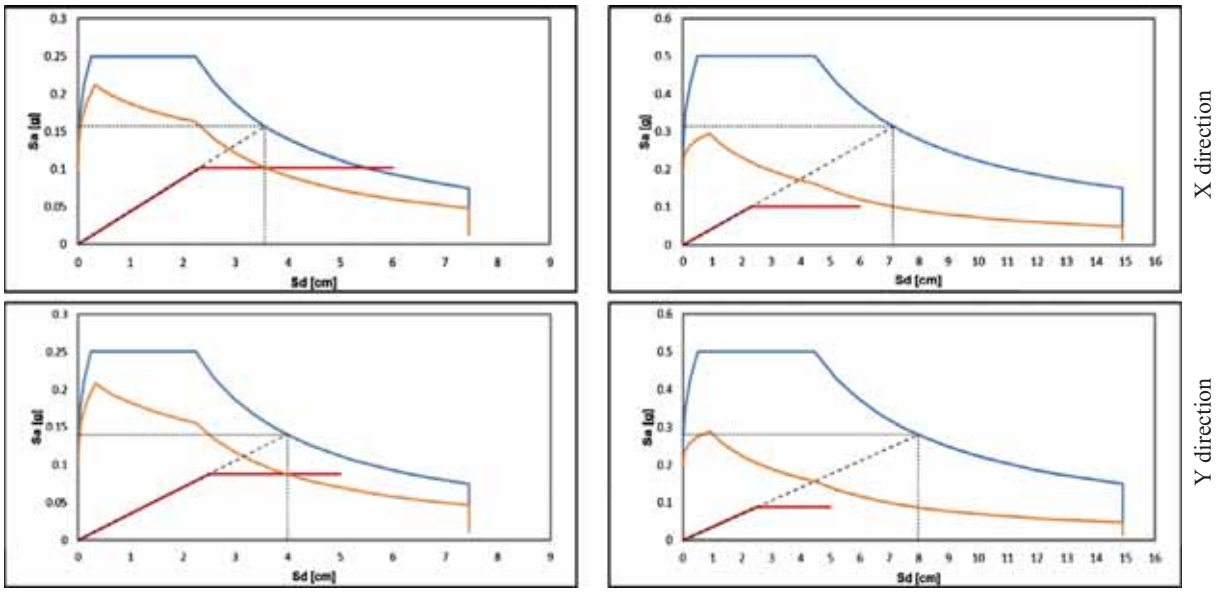

Fig. 19. Tower III: non-linear static procedure in the acceleration–displacement response spectrum plane for different seismic intensity levels (Sa_g = 0.1 g and Sa_g = 0.2 g).

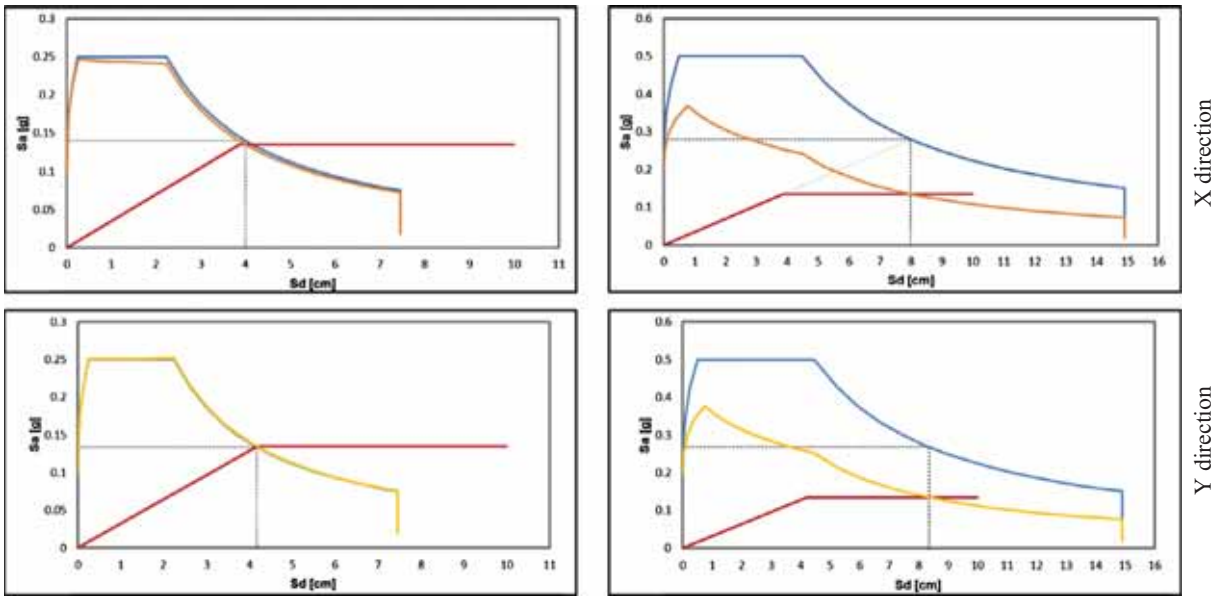

Fig. 20. Tower IV: non-linear static procedure in the acceleration–displacement response spectrum plane for different seismic intensity levels (Sa_g = 0.1 g and Sa_g = 0.2 g).

arrangement of the inner walls (T-shaped) and by the small openings in the walls in the *Y* direction.

The seismic demand (8 cm in the *X* direction and 8.35 cm in the *Y* direction) corresponding to Sa_g = 0.2 g is smaller than the capacity (9.95 cm in the *X* direction and 10.05 cm in the *Y* direction), which means that the verification of the tower is satisfied in terms of displacements for both the directions, see Fig. 20.

A clear damage distribution for vertical shear along the whole height of the tower is observed on all the walls, see Fig. 28. The damage pattern is affected by the presence of small openings and propagates along vertical lines.

5.1.5. Tower V

The pushover analyses show that the elastic stiffness of the system is similar for both the orthogonal directions. In terms of yield strength, the *Y* direction can be determined as the weakest one. Since the structure is symmetrical in plan, this difference can be explained by the presence of multiple openings on the walls in the *Y* direction. Another important characteristic of this tower is the presence of internal vaults on each floor, which may give a different behavior in the two orthogonal directions. The displacement demand (7.55 cm in the *X* direction and 8.2 cm in the *Y* direction) corresponding to Sa_g = 0.2 g is higher than the displacement capacity (7 cm in the *X* direction and 5 cm in the *Y* direction). The verification of the tower is not satisfied in terms of displacements for both the directions, see Fig. 21.

An inclined pattern of damage is clearly visible along the height of the tower, see Fig. 29. A damage concentration near the internal masonry vaults as a result of internal actions redistribution is also registered.

5.1.6. Tower VI

The pushover analyses indicate that the elastic stiffness and the yield strength of the system are smaller in the *X* direction. This

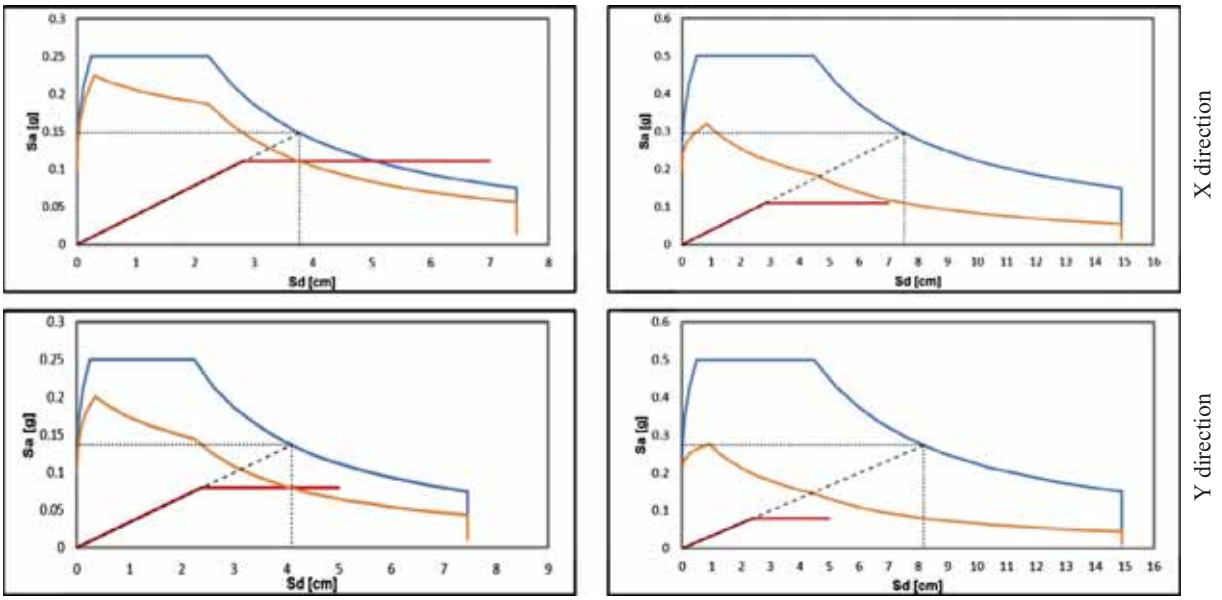

Fig. 21. Tower V: non-linear static procedure in the acceleration–displacement response spectrum plane for different seismic intensity levels (Sa_g = 0.1 g and Sa_g = 0.2 g).

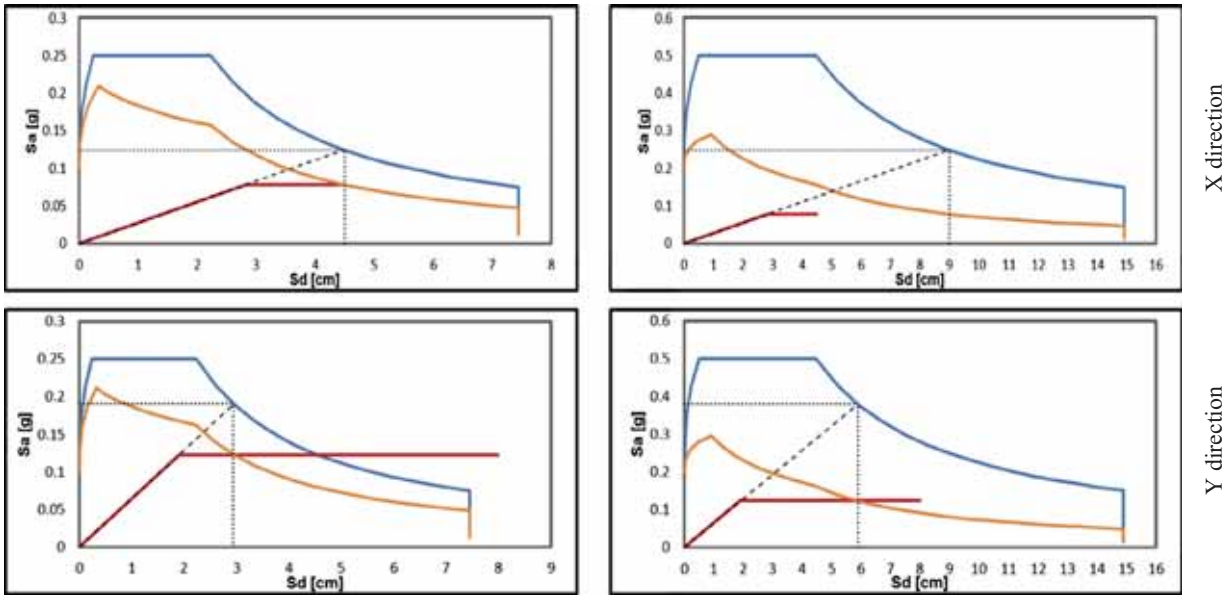

Fig. 22. Tower VI: non-linear static procedure in the acceleration–displacement response spectrum plane for different seismic intensity levels (Sa_g = 0.1 g and Sa_g = 0.2 g).

leads to the conclusion that the *X* direction is the weakest direction of this structure, as confirmed by the eigen-value analysis. This tower is not symmetrical in plan because one wall in the *X* direction is much thinner than the other walls. Moreover, the thin wall is characterized by multiple openings along the height and by a large arch on the top of the tower, which significantly reduces the structural stiffness. The displacement demand (9 cm) corresponding to Sa_g = 0.2 g is higher than the displacement capacity (4.5 cm) in the *X* direction, which means that the verification of the tower is not satisfied in terms of displacements in the *X* direction. It can be noted that for Sa_g = 0.1 g the displacement capacity and demand are very similar in the *X* direction, see Fig. 22.

A significant damage is clearly visible at the top of the tower above the big opening of the front wall, indicating a probable partial collapse of the most vulnerable part of the structure, see Fig. 30. Moreover, significant vertical damage is concentrated in the front wall characterized by small thickness and multiple openings, above all performing a pushover analysis in the *X* direction. Clear damage is also registered in the upper part of the back wall.

5.1.7. Tower VII

The pushover analyses confirm the results obtained from the eigen-value analysis, highlighting the different behavior in the two orthogonal directions. The structure is not symmetrical in plan and exhibits a quite relevant inclination in the negative *X* direction. The pushover curve presents smaller elastic stiffness and yield strength in the *X* direction. The displacement demand (8.6 cm) corresponding to Sa_g = 0.2 g is higher than the displacement capacity (5.1 cm), which means that the verification of the tower is not satisfied in terms of displacements in the *X* direction. For Sa_g = 0.2 g the displacement capacity and demand are very similar in the *Y* direction, see Fig. 23.

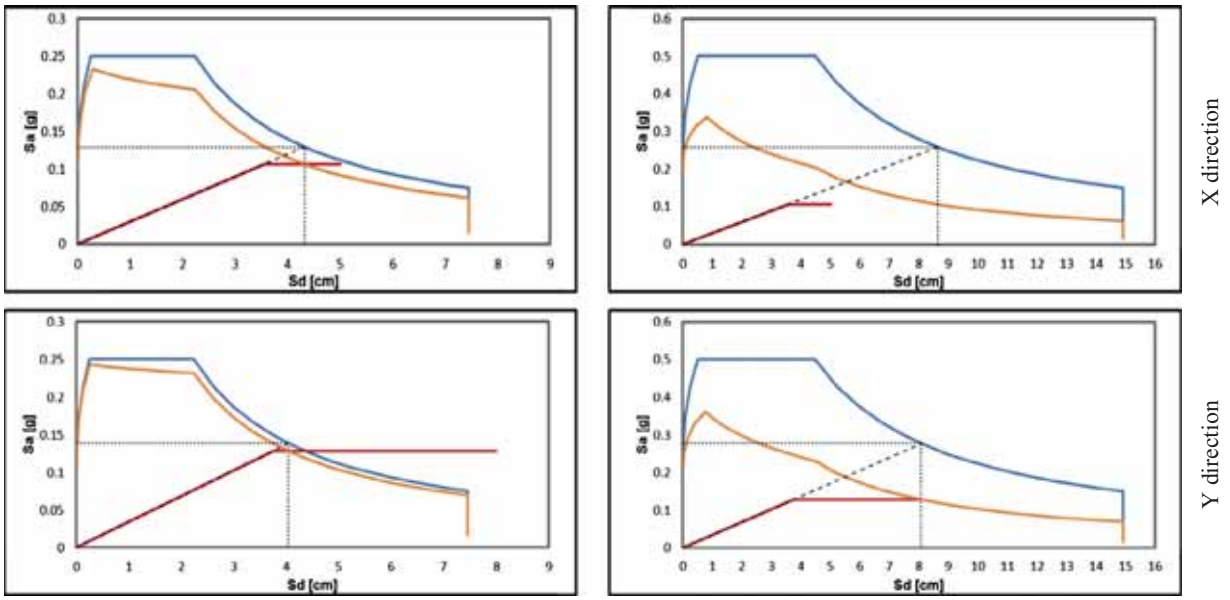

Fig. 23. Tower VII: non-linear static procedure in the acceleration–displacement response spectrum plane for different seismic intensity levels (Sa_g = 0.1 g and Sa_g = 0.2 g).

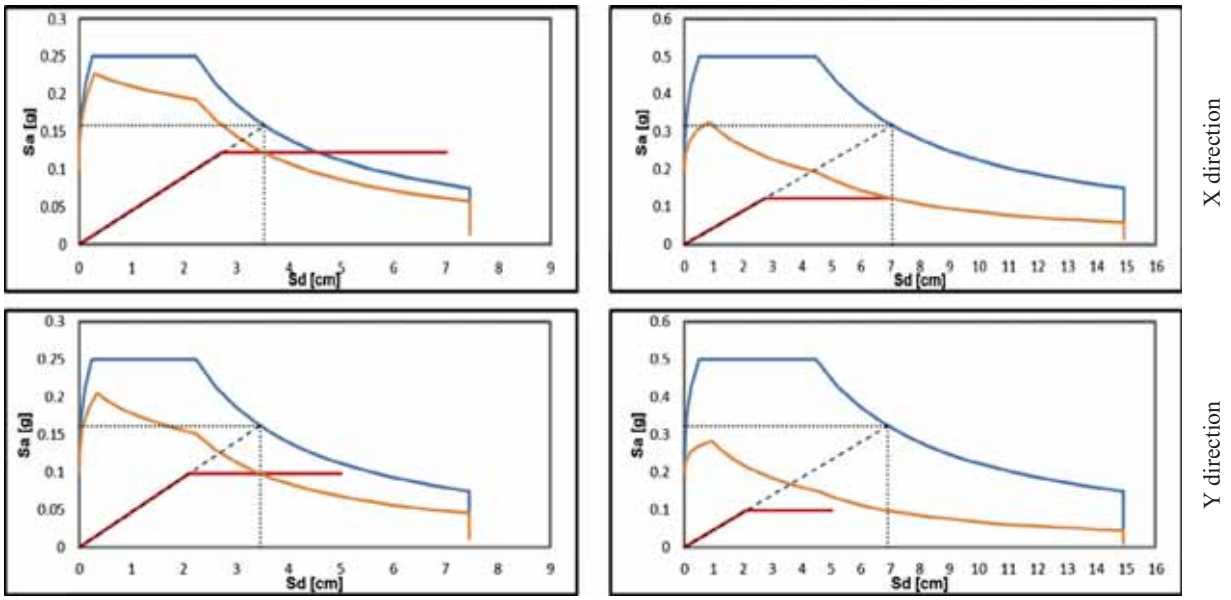

Fig. 24. Tower VIII: non-linear static procedure in the acceleration–displacement response spectrum plane for different seismic intensity levels (Sa_g = 0.1 g and Sa_g = 0.2 g).

During the pushover analysis in the *X* direction severe damage spreads in a limited portion of the tower near the base, see Fig. 31. From the results of the numerical simulations, it can be deduced that the inclination makes the structure quite vulnerable to damage.

5.1.8. Tower VIII

From a geometrical point of view, the tower is not symmetrical in plan and elevation, which leads to different stiffnesses in the two orthogonal directions. The pushover curve presents smaller yield strength in the *Y* direction. This can be explained by the arrangement of the internal wall and the presence of several openings on the walls in the *Y* direction. The displacement demand (6.9 cm) corresponding to Sa_g = 0.2 g is higher than the displacement capacity (5 cm) in the *Y* direction. The verification of the tower is not satisfied in terms of displacements in the *Y* direction, see Fig. 24. For Sa_g = 0.2 g the displacement demand is only slightly smaller than the capacity in the *X* direction, indicating that the structure is near a critical state.

The damage distribution is concentrated mainly near the openings along the whole height of the walls, see Fig. 32, and clear diffused damage is mainly observed on the walls in the *Y* direction.

From an overall analysis of the numerical predictions of the non-linear static procedure, it can be observed that the towers, except Tower VI, have the resources to satisfy the demand corresponding to Sa_g = 0.1 g for both the directions, whereas the majority are unsafe at least along one geometric direction for Sa_g = 0.2 g. Only Tower II and Tower IV are able to resist the seismic action corresponding to Sa_g = 0.2 g according to the non-linear static procedure.

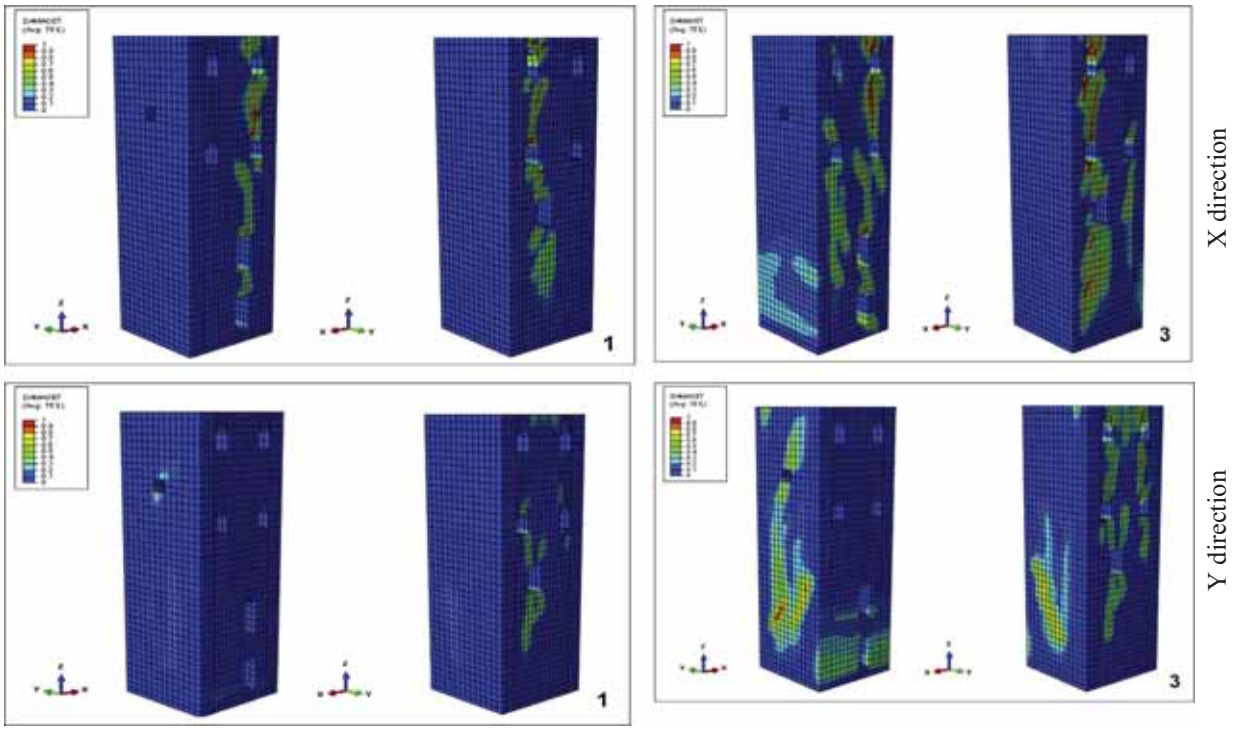

Fig. 25. Tensile damage distribution for Tower I in the *X* and *Y* directions at seismic demand equal to Sa_g = 0.1 g (left) and Sa_g = 0.2 g (right).

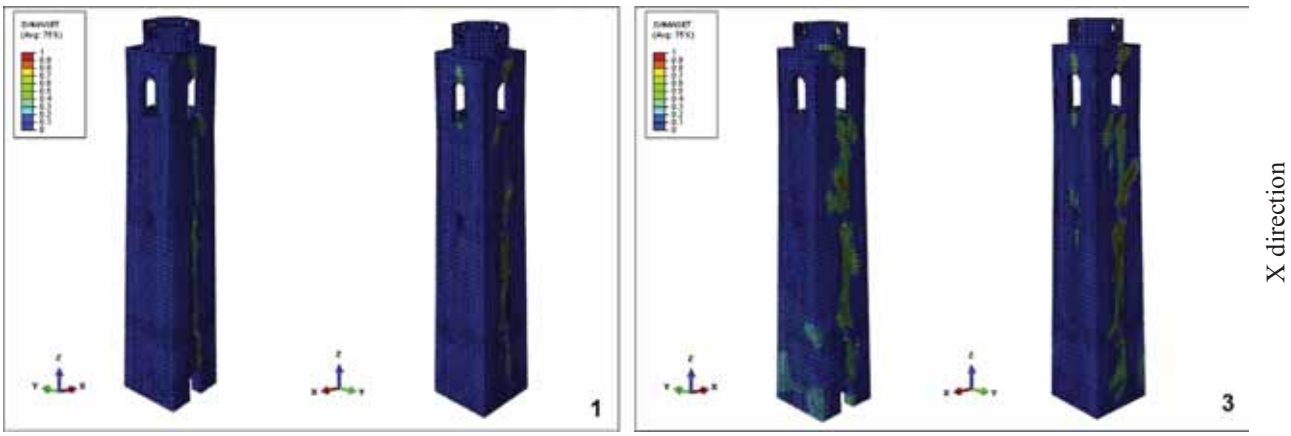

Fig. 26. Tensile damage distribution for Tower II in the *X* direction at seismic demand equal to Sa_g = 0.1 g (left) and Sa_g = 0.2 g (right).

6. Seismic safety Index and collapse acceleration

For the seismic performance assessment of the towers under study, a simplified sectional approach suggested by Italian Guidelines on the cultural heritage [3] is also performed. An equivalent static analysis is carried out, adopting a distribution of horizontal forces proportional to the product $W_i z_i$, being W_i the weight associated with the *i*th node and z_i its vertical position. In this study, in order to compare the results with the non-linear static procedure, reference is made to the elastic response spectrum provided by Eurocode 8 [4] with soil type C, reduced by the behavior factor q = 2.8, as suggested by Italian Guidelines in the case of stiffness irregularities along the height. According to Italian Guidelines, it is necessary to compare the acting bending moments with the resisting ones in different transversal sections, within the application of equivalent static loads. For towers with rectangular cross-section, detailed finite element analyses may be avoided and simplified formulas could be adopted according to Italian Guidelines requirements. A simplified mechanical model is assumed, schematizing the tower as a cantilever and performing the assessment at the base of each section under combined compressive and bending stresses. For towers with rectangular cross-section and under the assumption that the normal pre-compression does not exceed $0.85 f_d A_s$, the ultimate bending moment at the base is given by:

$$M_u = \frac{\sigma_0 A}{2}\left(b - \frac{\sigma_0 A}{0.85 a f_d}\right) \tag{7}$$

where a is the depth of the section in the direction of the seismic action, b is the width of the section in the orthogonal direction of the seismic action, A is the cross-section area, σ_0 = W/A is the average pre-compression (W is the tower weight above the section considered) and f_d is the design compressive strength of masonry. The acting bending moment may be evaluated by applying a system of lateral forces under the assumption of horizontal displacements increasing linearly along the height of the structure.

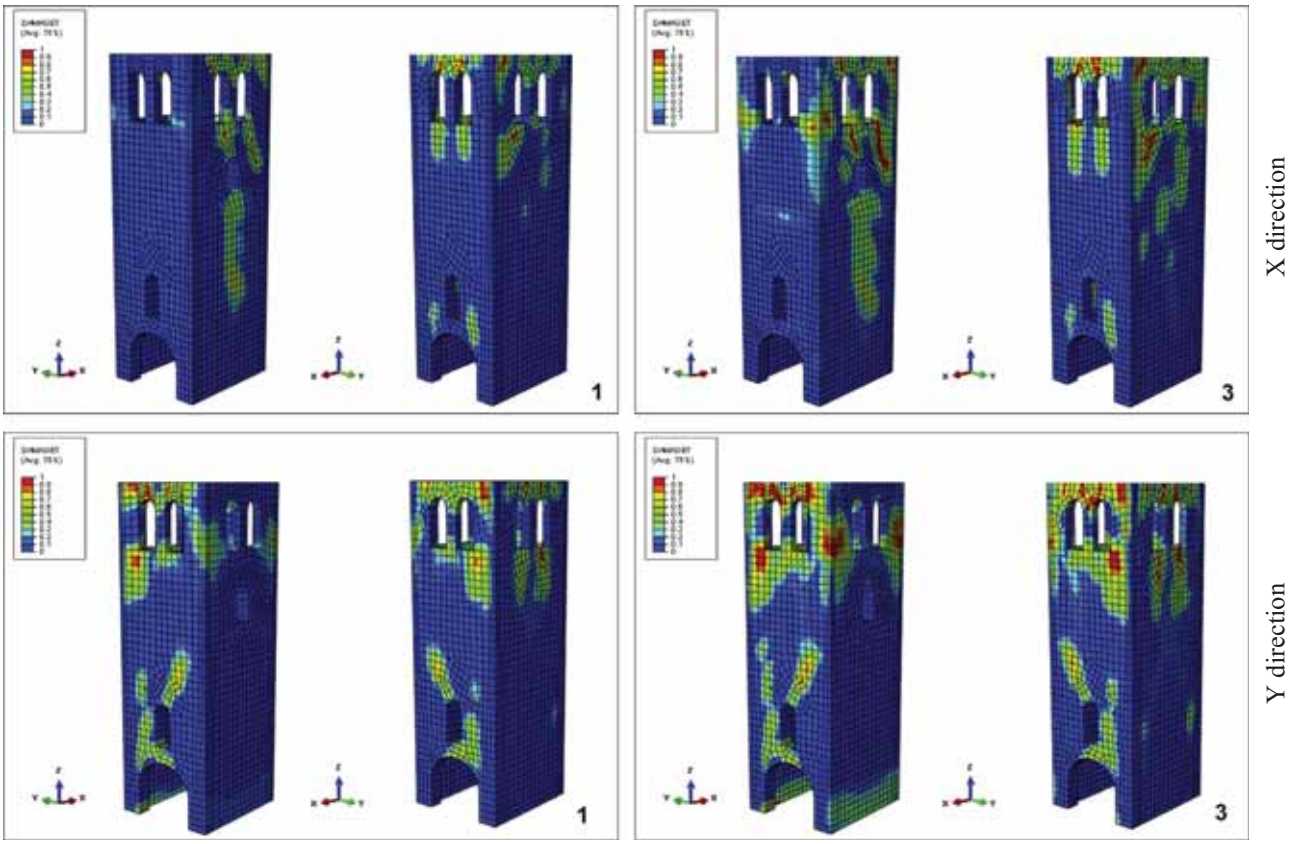

Fig. 27. Tensile damage distribution for Tower III in the *X* and *Y* directions at seismic demand equal to Sa_g = 0.1 g (left) and Sa_g = 0.2 g (right).

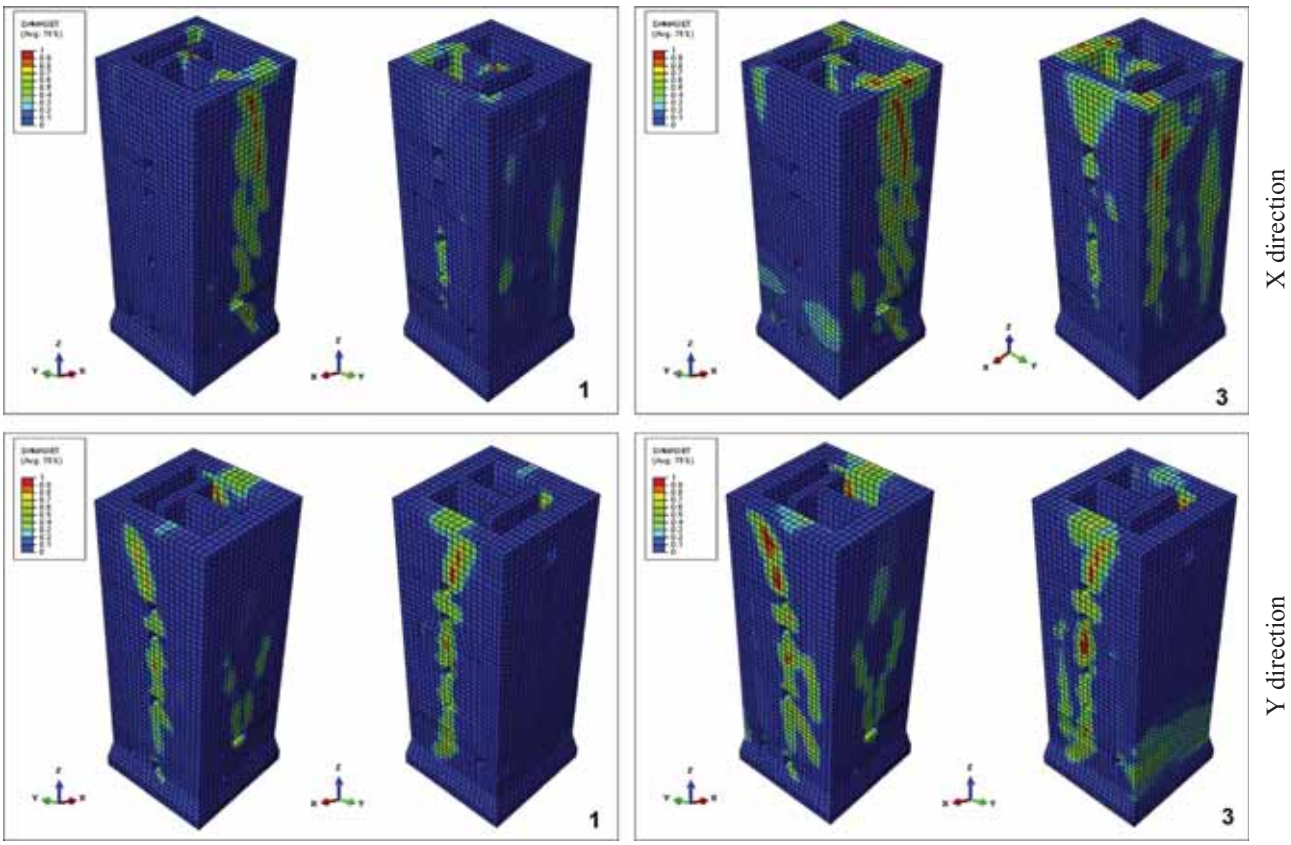

Fig. 28. Tensile damage distribution for Tower IV in the *X* and *Y* directions at seismic demand equal to Sa_g = 0.1 g (left) and Sa_g = 0.2 g (right).

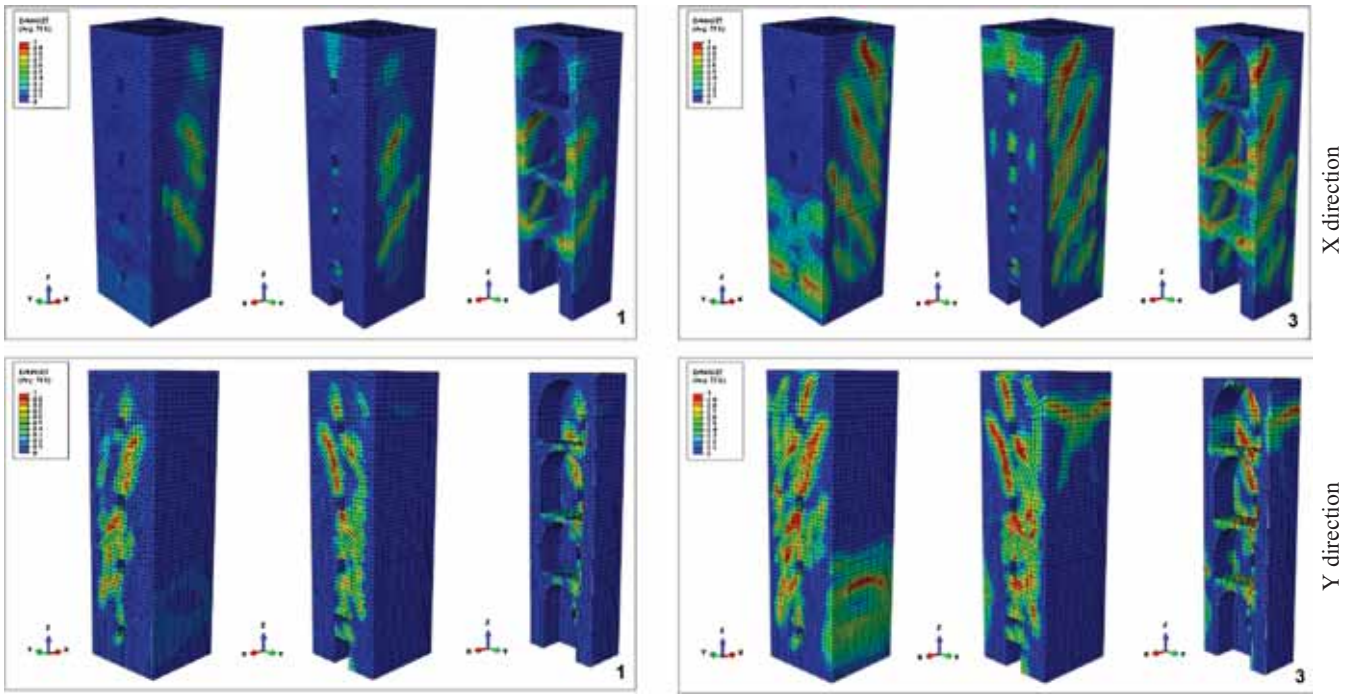

Fig. 29. Tensile damage distribution for Tower V in the *X* and *Y* directions at seismic demand equal to Sa_g = 0.1 g (left) and Sa_g = 0.2 g (right).

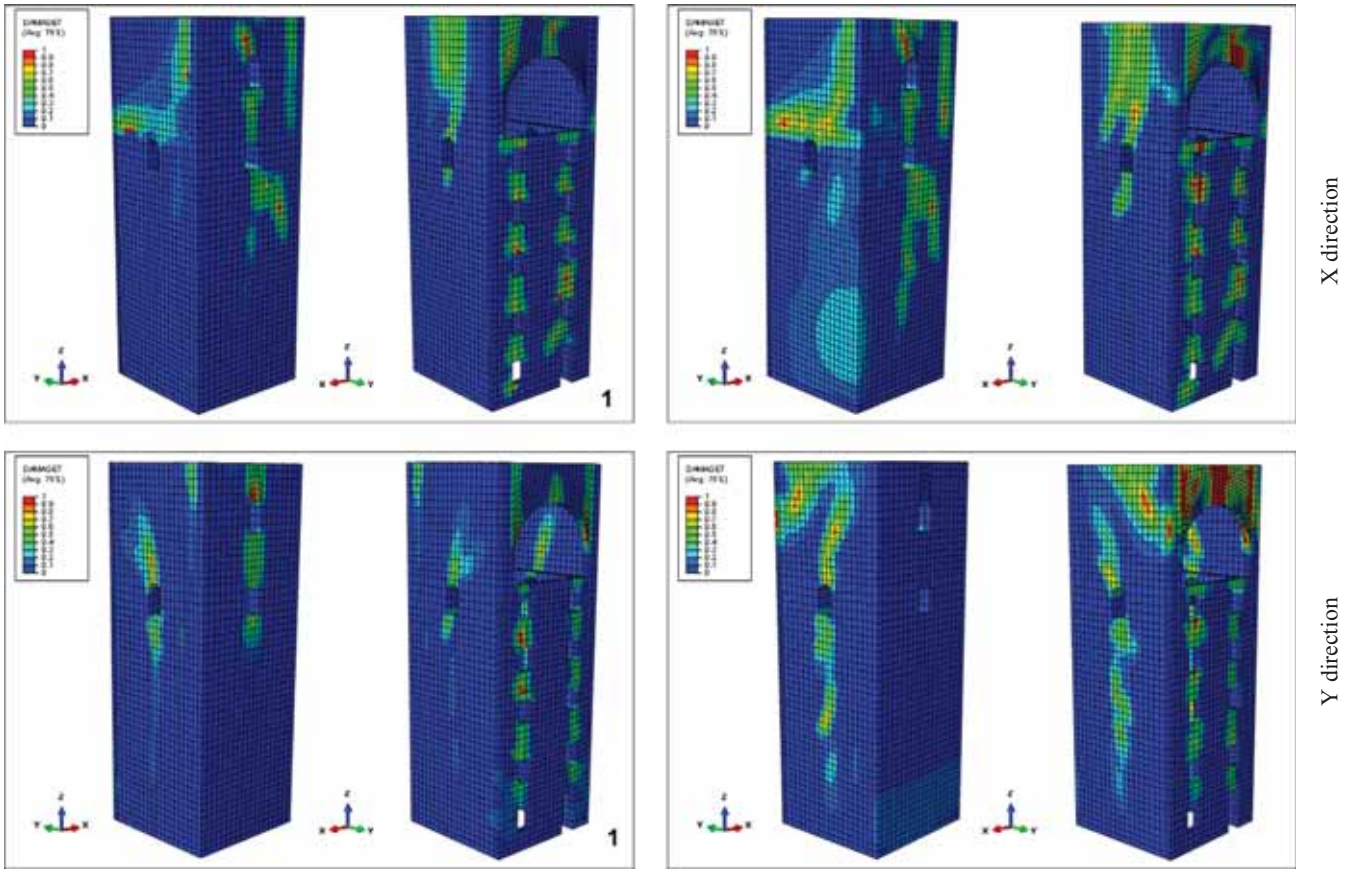

Fig. 30. Tensile damage distribution for Tower VI in the *X* and *Y* directions at seismic demand equal to Sa_g = 0.1 g (left) and Sa_g = 0.2 g (right).

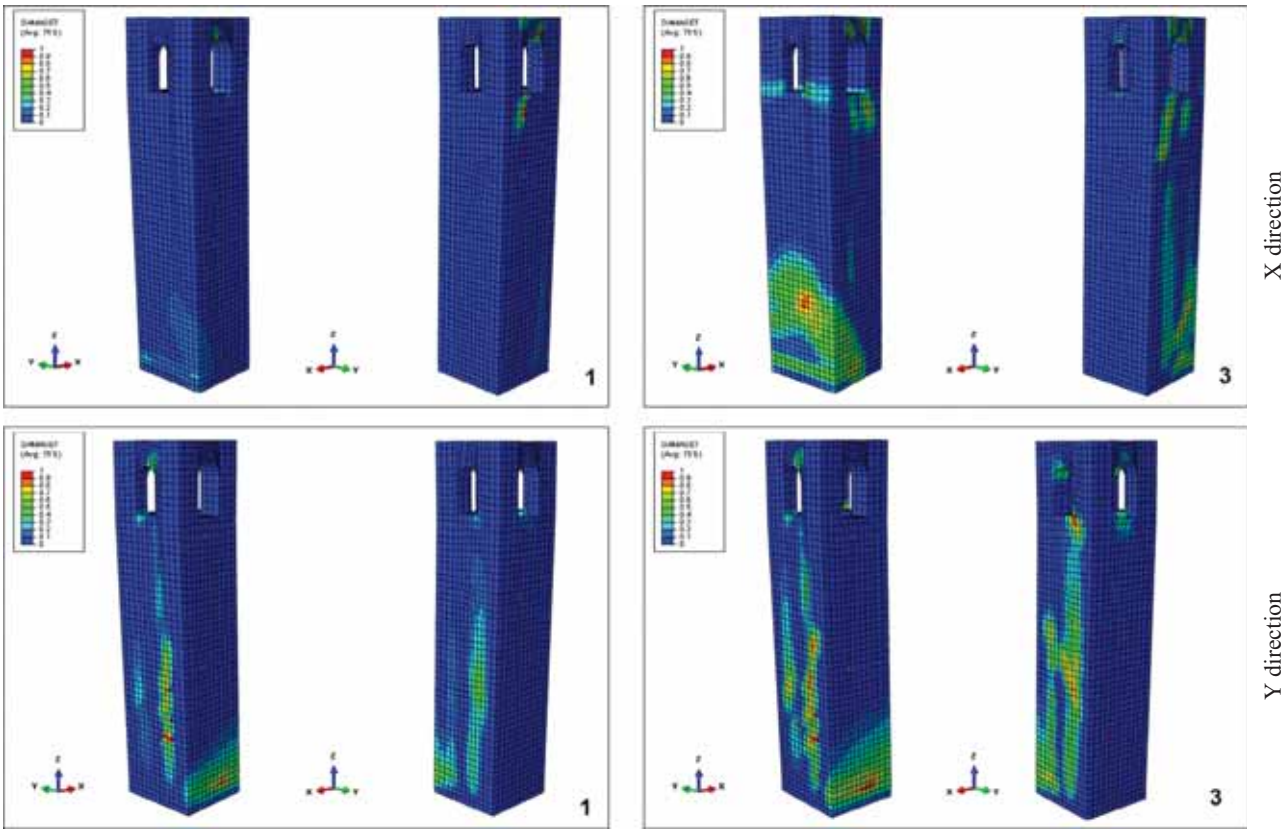

Fig. 31. Tensile damage distribution for Tower VII in the *X* and *Y* directions at seismic demand equal to Sa_g = 0.1 g (left) and Sa_g = 0.2 g (right).

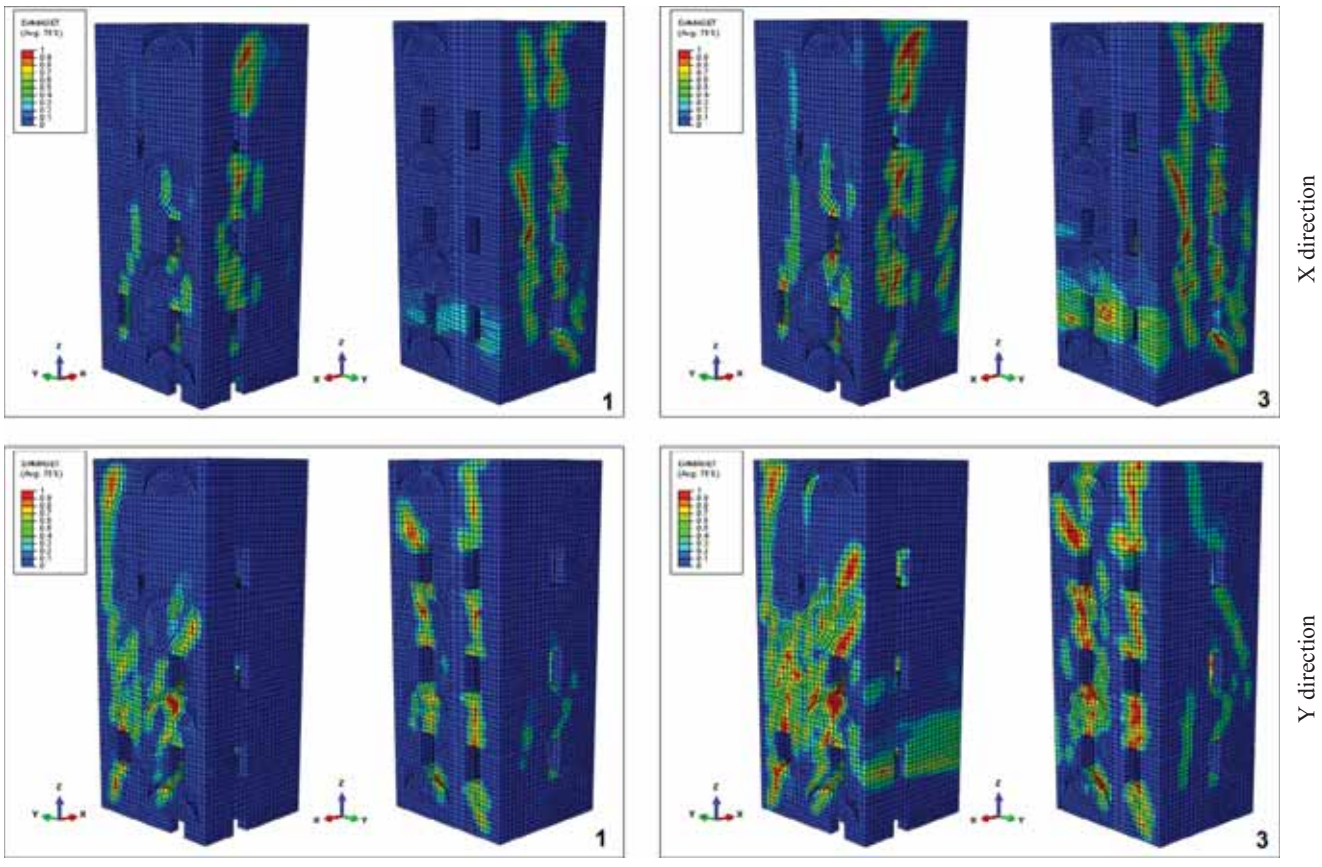

Fig. 32. Tensile damage distribution for Tower VIII in the *X* and *Y* directions at seismic demand equal to Sa_g = 0.1 g (left) and Sa_g = 0.2 g (right).

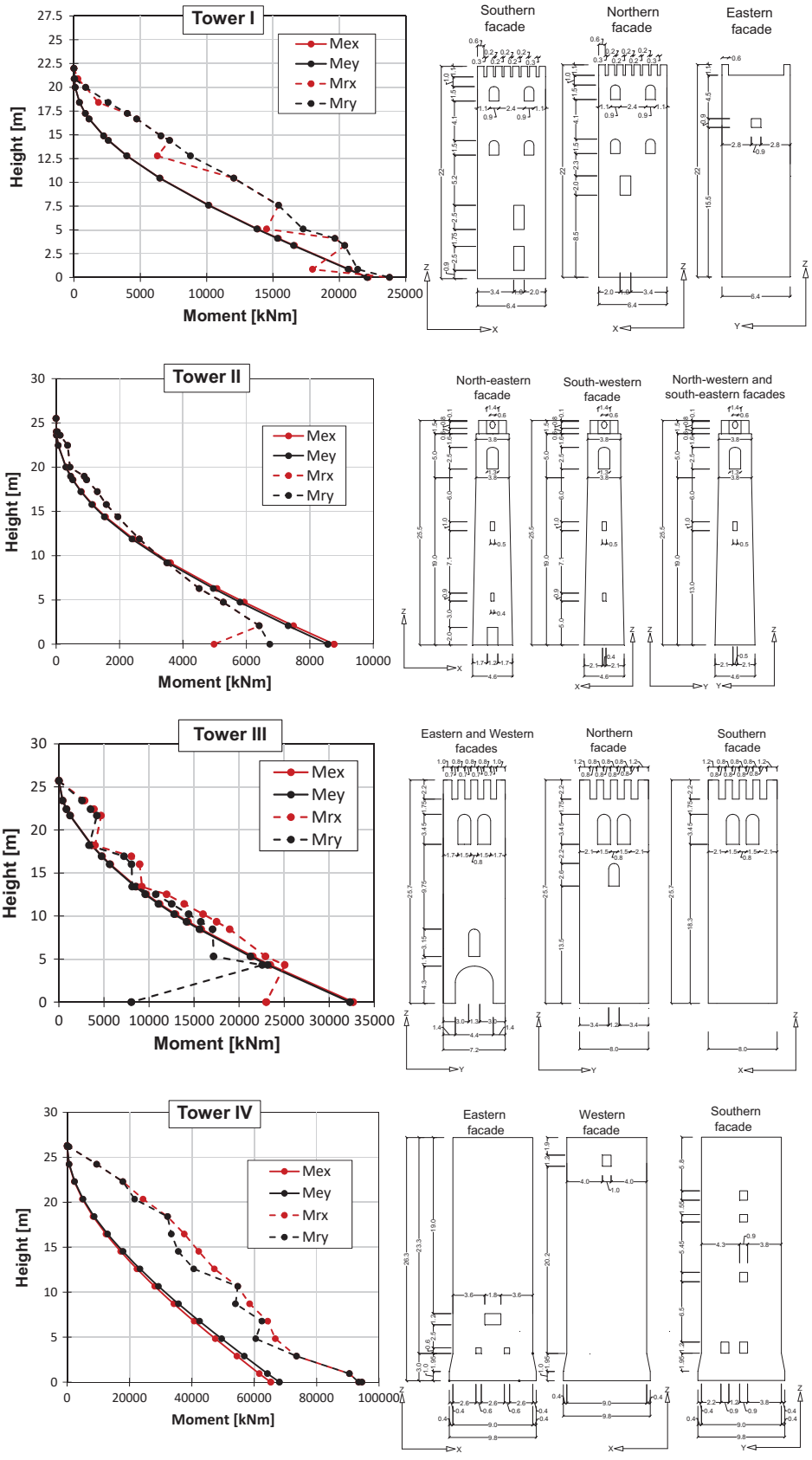

Fig. 33. Towers I–IV: values of the resistant and applied bending moments evaluated with the EC8 response spectrum in both the directions along the height of the different towers.

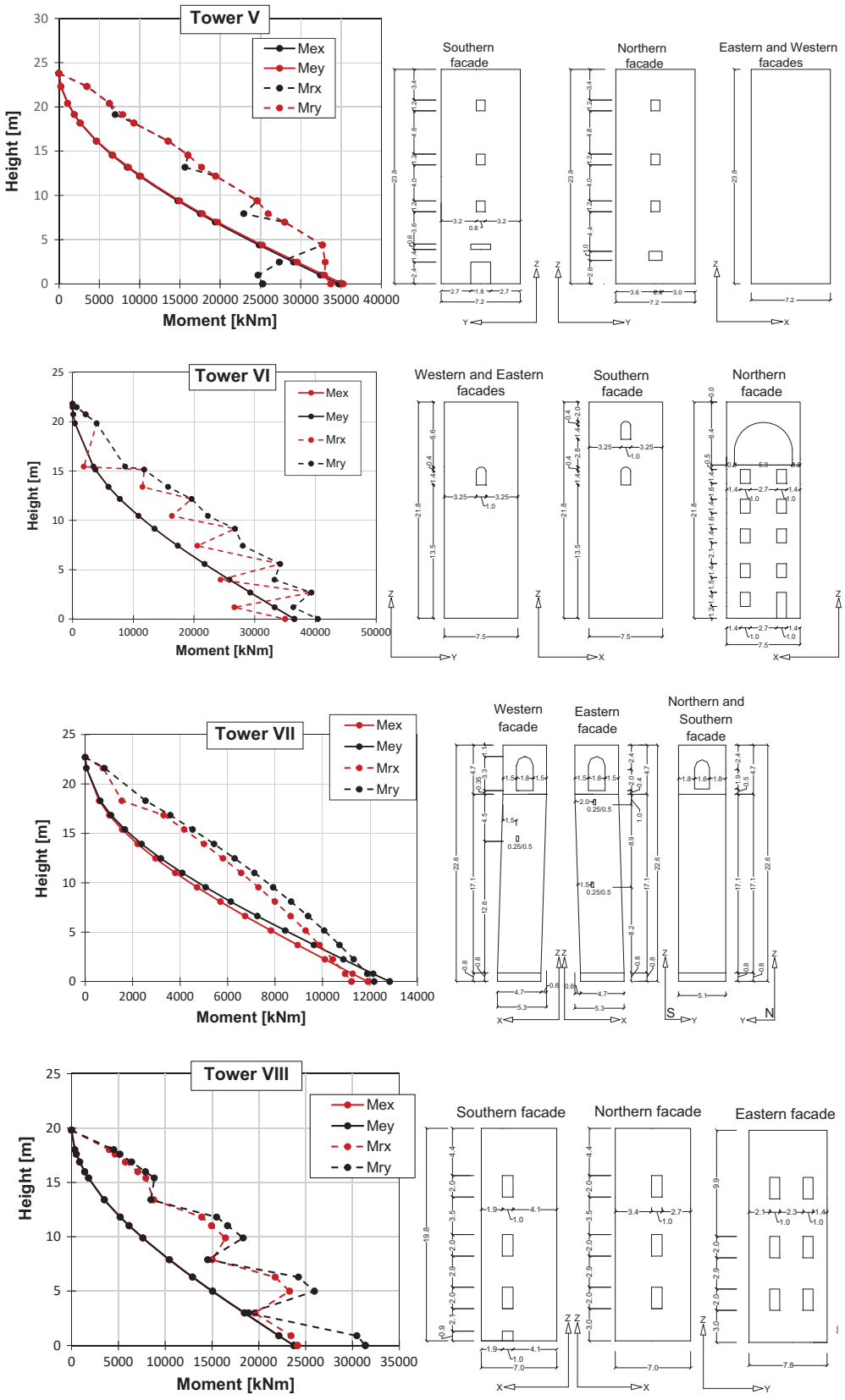

Fig. 34. Towers V–VIII: values of the resistant and applied bending moments evaluated with the EC8 response spectrum in both the directions along the height of the different towers.

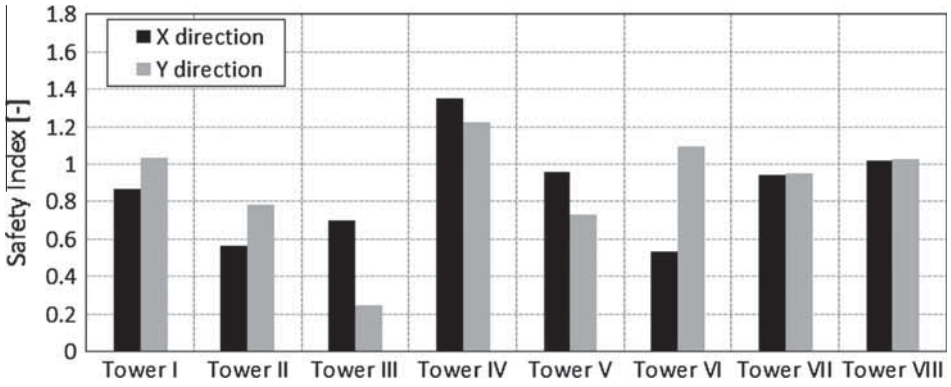

Fig. 35. Values of the Safety Index by Italian Guidelines procedure for the different towers in the *X* and *Y* directions.

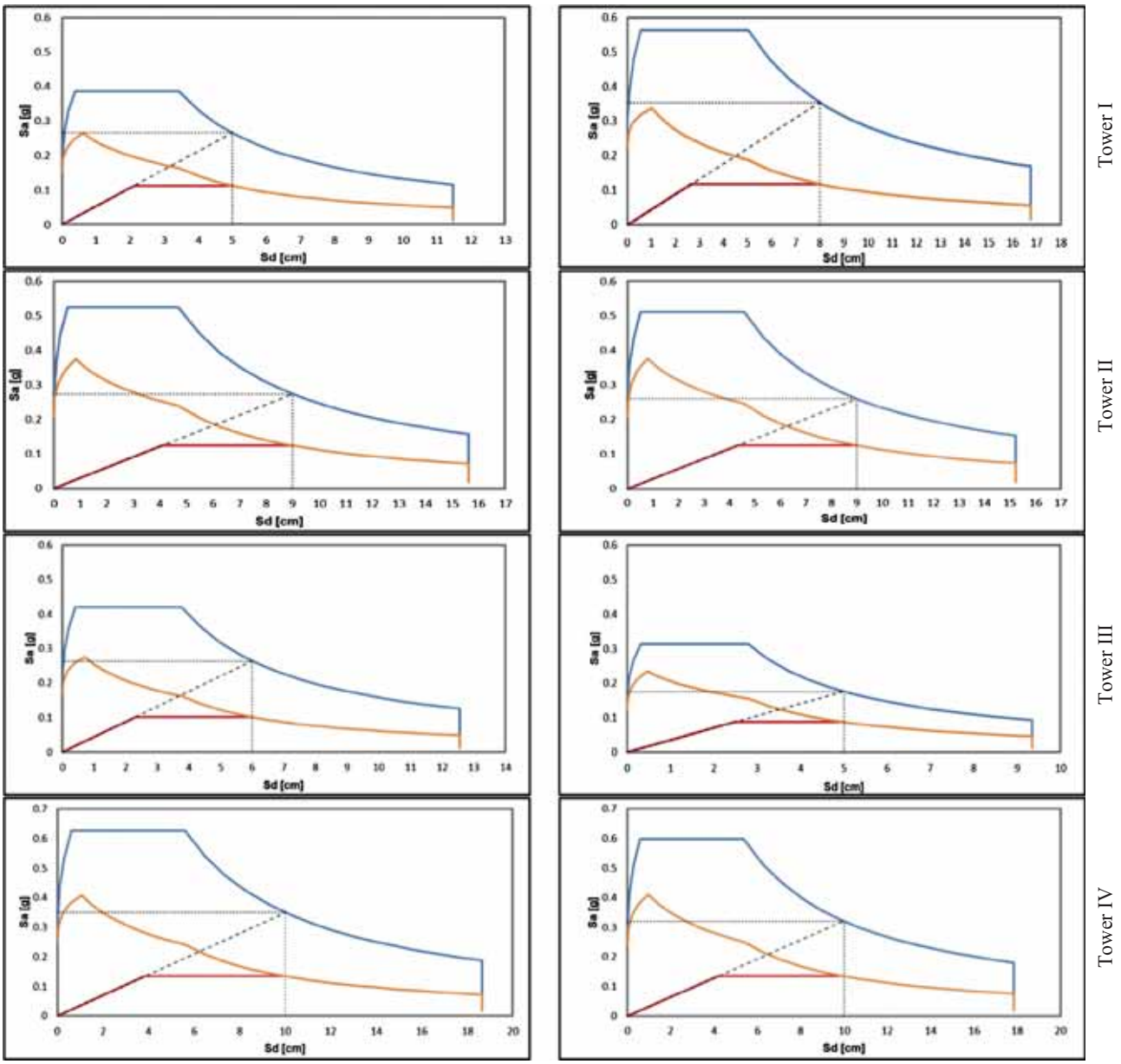

Fig. 36. Towers I–IV. Non-linear static procedure in the acceleration–displacement response spectrum plane: maximum peak ground acceleration supported by the towers in the *X* (left) and *Y* (right) directions.

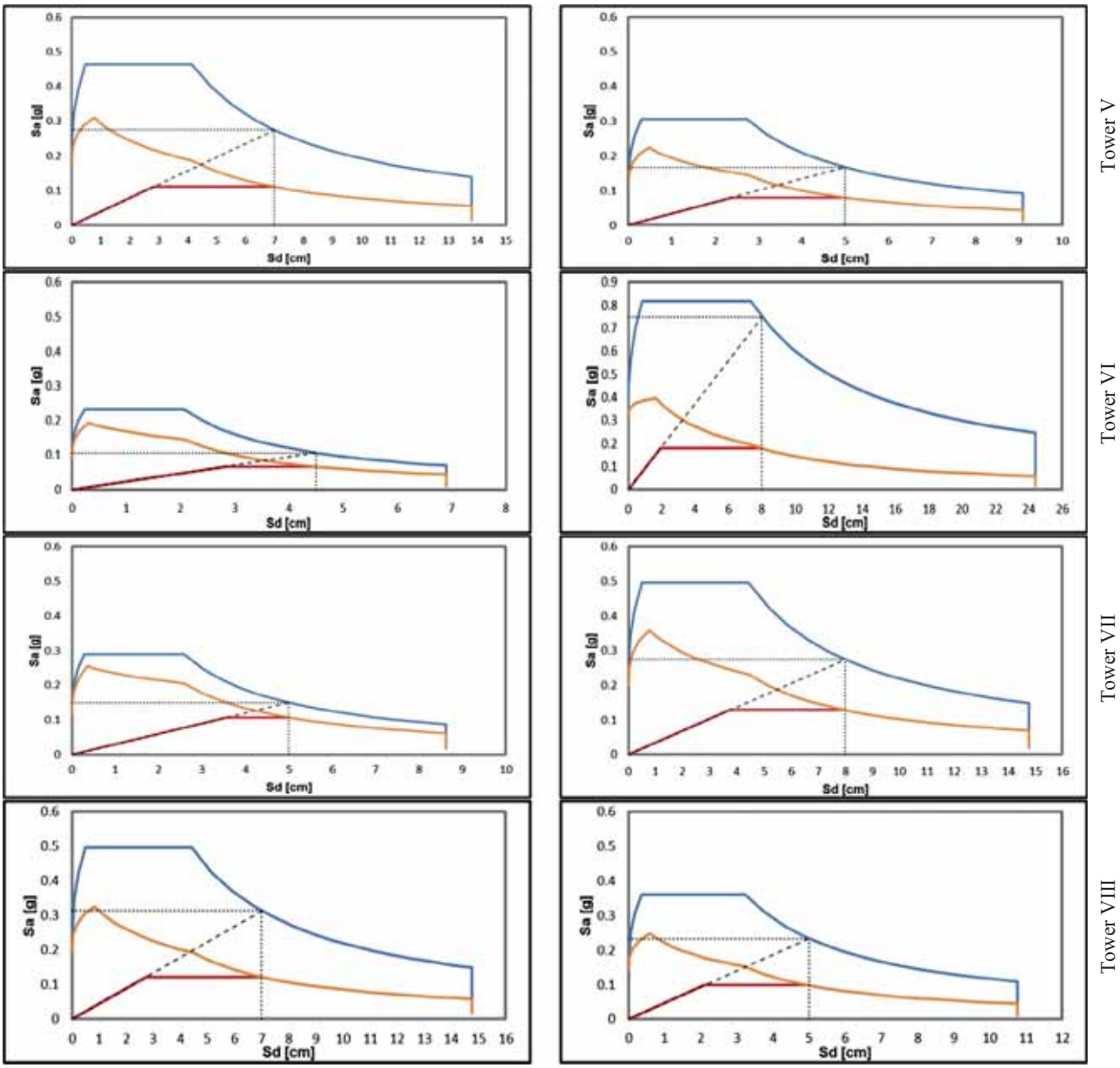

Fig. 37. Towers V–VIII. Non-linear static procedure in the acceleration–displacement response spectrum plane: maximum peak ground acceleration supported by the towers in the *X* (left) and *Y* (right) directions.

Figs. 33 and 34 show the resultant distributions of the resisting (Mr) and acting (Me) bending moments in the two orthogonal directions along the height of the different towers under study for a ground motion corresponding to $Sa_g = 0.2$ g. In particular, the results for Towers I–IV are reported in Fig. 33 and for Towers V-VIII in Fig. 34.

As can be noted, in the majority of cases the lower part of the towers exhibits insufficient strength for flexural actions. In some cases, the presence of some openings in the lower part of the tower weakens further the transversal section decreasing the resistance against flexural actions, which obviously reach the maximum value on the fixed base. The maximum difference between applied and resistant bending moments is registered for Tower III along *Y* direction because of the large openings at the base.

According to the simplified sectional approach suggested by the Italian Guidelines on Cultural Heritage, the seismic safety Index is evaluated for the towers under consideration. The seismic safety Index can be defined as follows:

$$I_s = \frac{a_{SLU}}{a_g} \tag{8}$$

where a_{SLU} is the peak ground acceleration corresponding to the collapse of the structure and a_g the design ground acceleration on ground type A. A value of the seismic safety Index I_s greater than one corresponds to a safe state for the tower under consideration. This index may be useful for an evaluation of the weakness of the structure in terms of strength.

The values of the seismic safety Index I_S obtained for the eight towers analyzed are reported in Fig. 35 for $Sa_g = 0.2$ g. The seismic safety Index I_S is smaller than one for almost all the towers, except for Tower IV and Tower VIII, meaning that the seismic vulnerability of the towers is higher than the limit required by the code.

6.1. Comparison in terms of collapse acceleration

Figs. 36 and 37 illustrate the determination of the seismic capacity of the different towers along both the *X* and *Y* directions

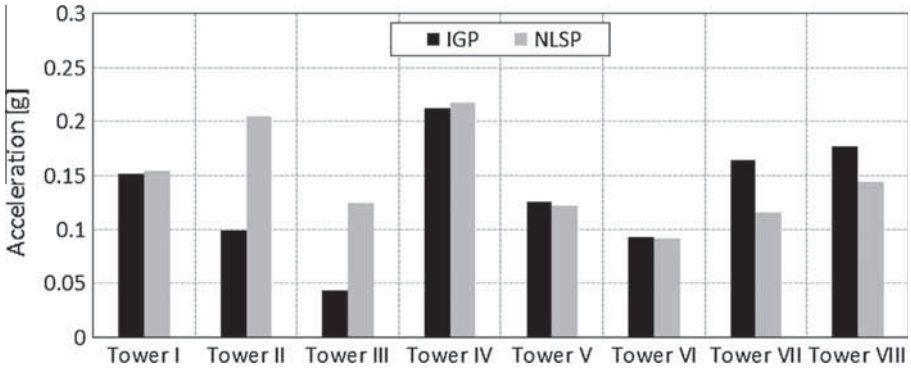

Fig. 38. Values of the collapse acceleration found by Italian Guidelines procedure and non-linear static procedure for the different towers.

in the acceleration–displacement response spectrum plane according to the non-linear static procedure. The seismic capacity is evaluated in terms of the maximum value of the peak ground acceleration that the tower can withstand and the demand spectrum at which the seismic demand is equal to the capacity is shown. The seismic capacities of the different towers in terms of maximum peak ground acceleration are summarized in Fig. 38, where the collapse accelerations obtained by means of the simplified sectional approach proposed by Italian Guidelines are also reported. It can be seen that both the procedures indicate that Tower IV is able to withstand the largest ground motion intensity. The seismic capacity of Tower IV, in terms of peak ground acceleration, amounts to about 0.2 g. It is found that the results obtained with the two different procedures are generally in a good agreement, except for Tower II and Tower III, for which the simplified sectional approach proposed by Italian Guidelines indicates smaller values of the maximum peak ground accelerations. Tower II presents the highest value of slenderness and Tower III exhibits large openings at the base in one direction.

As can be observed, in some cases there are some evident discrepancies between the results obtained from the non-linear static procedure and the simplified sectional approach. This is mainly linked to the fact that the Italian code approach is basically conceived thinking about the equivalence with a cantilever beam, where failure occurs exclusively for the formation of a flexural hinge near the base. All those failures related to different collapse modes, such as shear failure or collapse near the top due to squat geometries, presence of irregularities, high perforations and bell towers, cannot be properly taken into account with the procedure envisaged by Italian Guidelines on Cultural Heritage [3].

7. Conclusions

The assessment of the seismic performance of eight historical masonry towers, located in the North-East region of Italy, is carried out by means of simplified approaches. From an overall analysis of the results obtained in this study, the following remarks can be made.

- Preliminary eigen-frequency analyses may provide some basic information about the dynamic characteristics of the different towers. Albeit approximate, because masonry exhibits a non-linear behavior even at very low levels of seismic excitation, such a standard approach may give a rough indication of the weaknesses of the structures that can be compared with more sophisticated methods of analysis. Standard eigen-frequency analysis allows identifying – among other results and in the framework of linear elasticity – the vibration modes characterized by a high participating mass as well as the corresponding periods to compare with accelerations provided by code response spectra.
- A simplified procedure based on non-linear static pushover analyses is adopted for the seismic verification of the global performance of the eight towers. The assessment of the global structural response is carried out in the case of a ground motion corresponding to different values of the peak ground acceleration (Sa_g = 0.1 g and Sa_g = 0.2 g) with reference to the response spectrum provided by Eurocode 8 with ground type C, comparing displacement demand and capacity. It can be observed that the towers under study, except Tower VI, have the resources to satisfy the seismic demand for Sa_g = 0.1 g in both the directions, whereas the majority are not verified at least along one geometric direction for Sa_g = 0.2 g. Only Tower II and Tower IV are able to resist the seismic action for Sa_g = 0.2 g.
- The evaluation of the seismic safety Index by means of the simplified sectional approach suggested by Italian Guidelines on Cultural Heritage is also presented. A quite regular trend of the results is observed for the towers in dependence of the height, large openings, walls thickness, cross-section area and presence of irregularities or internal vaults. In the majority of the cases the lower part of the towers exhibits insufficient strength due to the presence of some openings that weaken further the transversal section, decreasing the resistance against flexural actions.
- The collapse accelerations obtained through the non-linear static procedure and the simplified sectional approach suggested by Italian Guidelines for the different towers are evaluated and compared. It is found that the results obtained with the different procedures fit reasonably well, with a slight conservative trend for the simplified approach proposed by Italian Guidelines.

A comparison of the results obtained through the simplified approaches used in this study with non-linear dynamic analyses is presented in a companion paper of the authors, [31].

To conclude, it should be noted that the eight towers investigated in this study represent a small but meaningful sample extracted from an almost infinite database of cases that can be encountered in practice. Obviously, a systematic analysis – albeit very detailed - on only eight towers does not allow for drawing general conclusions, but may help to provide predictive qualitative information on the expected seismic behavior. Intuition suggests that the most important geometric parameters characterizing the structural behavior of a tower may be slenderness, shear area of transversal sections and regularity/irregularity along the height. Generally speaking and simply in agreement with intuition, it can be affirmed that on the basis of the present simulations slender towers tend to behave similarly to Euler–Bernoulli cantilevers (forming a flexural hinge near the base at failure), whereas, in the presence of large areas of transversal sections, collapse is obviously more related to shear. The role played by structural

irregularities, including in particular the cases where stiff stairs, internal vaults and large openings are present, is hardly predictable and should be taken into account carefully case by case.

References

[1] DM 14/01/2008. Nuove norme tecniche per le costruzioni. Ministero delle Infrastrutture (GU n.29 04/02/2008), Rome, Italy. [New technical norms on constructions].

[2] Circolare n 617 del 2 febbraio 2009. Istruzioni per l'applicazione delle nuove norme tecniche per le costruzioni di cui al decreto ministeriale 14 gennaio 2008. [Instructions for the application of the new technical norms on constructions].

[3] DPCM 9/2/2011. Linee guida per la valutazione e la riduzione del rischio sismico del patrimonio culturale con riferimento alle Norme tecniche delle costruzioni di cui al decreto del Ministero delle Infrastrutture e dei trasporti del 14 gennaio 2008. [Italian Guidelines for the evaluation and reduction of the seismic risk of Cultural Heritage, with reference to the Italian norm of constructions].

[4] Comite Europeen de Normalisation (2004). Eurocode 8 EN1998-1 and EN1998-3: Design of structures for earthquake resistance. CEN, Brussels.

[5] F. Doglioni, V. Petrini, A. Moretti, Le chiese e il terremoto [Churches and earthquake], LINT Press, Trieste, Italy, 1994.

[6] S. Casolo, G. Milani, G. Uva, C. Alessandri, Comparative seismic vulnerability analysis on ten masonry towers in the coastal Po valley in Italy, Eng. Struct. 49 (2013) 465–490.

[7] G. Milani, M. Valente, Comparative pushover and limit analyses on seven masonry churches damaged by the 2012 Emilia-Romagna (Italy) seismic events: possibilities of non-linear Finite Elements compared with pre-assigned failure mechanisms, Eng. Failure Anal. 47 (2015) 129–161.

[8] G. Milani, M. Valente, Failure analysis of seven masonry churches severely damaged during the 2012 Emilia-Romagna (Italy) earthquake: non-linear dynamic analyses vs conventional static approaches, Eng. Failure Anal. 54 (2015) 13–56.

[9] M. Acito, M. Bocciarelli, C. Chesi, G. Milani, Collapse of the clock tower in finale emilia after the may 2012 emilia romagna earthquake sequence: numerical insight, Eng. Struct. 72 (2014) 70–91.

[10] E. Curti, S. Lagomarsino, S. Podestà, Dynamic models for the seismic analysis of ancient bell towers, in: P.B. Lourenço, P. Roca, C. Modena, S. Agrawal (Eds.), Proc. Structural Analysis of Historical Constructions SAHC-2006, MacMillan, New Delhi, India, 2006.

[11] A. Carpinteri, S. Invernizzi, G. Lacidogna, Numerical assessment of three medieval masonry towers subjected to different loading conditions, Masonry Int. 19 (2006) 65–75.

[12] P. Riva, F. Perotti, E. Guidoboni, E. Boschi, Seismic analysis of the Asinelli tower and earthquakes in Bologna, Soil Dyn. Earthquake Eng. 17 (1998) 525–550.

[13] K. Bernardeschi, C. Padovani, G. Pasquinelli, Numerical modelling of the structural behavior of Buti's bell tower, J. Cult. Heritage 5 (2004) 371–378.

[14] F. Peña, P.B. Lourenço, N. Mendez, D. Oliveira, Numerical models for the seismic assessment of an old masonry tower, Eng. Struct. 32 (2010) 1466–1478.

[15] A. Bayraktar, A. Sahin, M. Özcan, F. Yildirim, Numerical damage assessment of Haghia Sophia bell tower by nonlinear FE modeling, Appl. Math. Modell. 34 (2010) 92–121.

[16] G. Milani, S. Casolo, A. Naliato, A. Tralli, Seismic assessment of a medieval masonry tower in Northern Italy by limit, nonlinear static, and full dynamic analyses, Int. J. Archit. Heritage 6 (5) (2012) 489–524.

[17] S. Casolo, A three dimensional model for vulnerability analyses of slender masonry Medieval towers, J. Earthquake Eng. 2 (4) (1998) 487–512.

[18] J. Novak, J. Zeman, M. Sejnoha, J. Sejnoha, Pragmatic multi-scale and multi-physics analysis of Charles Bridge in Prague, Eng. Struct. 30 (11) (2008) 3365–3376.

[19] J. Sejnoha, M. Sejnoha, J. Zeman, J. Sykora, J. Vorel, Mesoscopic study on historic masonry, Struct. Eng. Mech. 30 (1) (2008) 99–117.

[20] J. Zeman, M. Sejnoha, From random microstructures to representative volume elements (2007), Modell. Simul. Mater. Sci. Eng. 15 (4) (2007) 5325–5335.

[21] M. Valente, Seismic upgrading strategies for non-ductile plan-wise irregular R/C structures, Proc. Eng. 54 (2013) 539–553.

[22] M. Valente, Seismic response of steel buildings with different structural typology, Appl. Mech. Mater. 256–259 (2013) 2234–2239.

[23] M. Valente, Seismic strengthening of non-ductile R/C structures using infill wall or ductile steel bracing, Adv. Mater. Res. 602–604 (2013) 1583–1587.

[24] M. Valente, Seismic rehabilitation of a three-storey R/C flat-slab prototype structure using different techniques, Appl. Mech. Mater. 193–194 (2012) 1346–1351.

[25] ABAQUS®, Theory Manual, Version 6.14.

[26] A.W. Page, The biaxial compressive strength of brick masonry, in: Proc. Instn Civ. Engrs, Part 2, 71, 1981, 893–906.

[27] G. Milani, P.B. Lourenco, A. Tralli, Homogenised limit analysis of masonry walls. Part I: failure surfaces, Comput. Struct. 84 (3–4) (2006) 166–180.

[28] R. Van der Pluijm, Shear behavior of bed joints, in: Proceedings of the 6th North American Masonry Conference. Philadelphia, Pennsylvania, USA, 6–9 June, 1993, 125–136.

[29] J. Lubliner, J. Oliver, S. Oller, E.A. Onate, A plastic-damage model for concrete, Int. J. Solids Struct. 25 (3) (1989) 299–326.

[30] P. Fajfar, A nonlinear analysis method for performance-based seismic design, Earthquake Spectra 16 (3) (2000) 573–592.

[31] M. Valente, G. Milani, Non-linear dynamic and static analyses on eight historical masonry towers in the North-East of Italy. Submitted and under revision, 2015.

[32] G. Milani, Simple homogenization model for the non-linear analysis of in-plane loaded masonry walls, Comput. Struct. 89 (2011) 1586–1601.

[33] G. Milani, Simple lower bound limit analysis homogenization model for in- and out-of-plane loaded masonry walls, Constr. Build. Mater. 25 (2011) 4426–4443.